

A compendium of photon emission rates, absorption cross sections and scattering cross sections

Rainer Dick*

*Department of Physics and Engineering Physics, University of Saskatchewan,
116 Science Place, Saskatoon, Canada SK S7N 5E2*

We provide a compendium of the quantum mechanical equations for photon emission rates, photon absorption cross sections, and photon scattering cross sections. For each case, the different equations that apply for discrete or continuous electron states of the emitting, absorbing, or scattering material are given.

Keywords: Photon emission, photon absorption, photon scattering, Kramers-Heisenberg formula

I. INTRODUCTION

Photons can be emitted, absorbed, or scattered in materials. Furthermore, the initial and final quantum states in atoms, molecules or condensed materials can be discrete or continuous. This allows for twelve different kinds of basic quantum optical transitions, and each of these kinds of transitions are described by their own quantum mechanical formulae.

The relevant techniques to derive the formulae involve second quantization and time-dependent perturbation theory, which are described in textbooks on advanced quantum mechanics, see e.g. [1–5]. These techniques are applied to the quantum optics Hamiltonian to derive amplitudes for photon emission, absorption and scattering. However, our focus in the present paper is not a review of the pertinent theoretical techniques, but rather to provide a concise list of the resulting photon emission rates, absorption cross sections, and scattering cross sections in the cases where photon-matter interactions are dominated by minimal coupling between photons and non-relativistic electrons. We will therefore only very briefly review the quantum optics Hamiltonian in Eqs. (1-6). Readers who are not interested in these details may very well skip Eqs. (1-5) and only take note that the results collected in this compendium are derived from the standard electron-photon coupling terms (6).

The description of photon processes in many-particle systems requires the use of quantized electromagnetic potentials for the photons and quantized matter fields $\Psi(\mathbf{x}, t)$ for the charged particles, and therefore a field-theoretic formulation of the Hamiltonian. The quantum optics Hamiltonian in Coulomb gauge, $\nabla \cdot \mathbf{A}(\mathbf{x}, t) = 0$, takes the form [5]

$$H = \int d^3\mathbf{x} \left(\sum_a \mathcal{H}_a(\mathbf{x}, t) + \mathcal{H}_\gamma(\mathbf{x}, t) + \sum_a \mathcal{H}_{a\gamma}(\mathbf{x}, t) \right) + \int d^3\mathbf{x} \int d^3\mathbf{x}' \sum_{ab} \mathcal{H}_{ab}(\mathbf{x}, \mathbf{x}', t). \quad (1)$$

Here

$$\mathcal{H}_a(\mathbf{x}, t) = \sum_s \frac{\hbar^2}{2m_a} \nabla \Psi_{a,s}^+(\mathbf{x}, t) \cdot \nabla \Psi_{a,s}(\mathbf{x}, t) \quad (2)$$

is the kinetic term for particles of species a (electrons and atomic nuclei) with mass m_a and electric charge q_a , and s is a spin orientation label. Furthermore,

$$\mathcal{H}_\gamma(\mathbf{x}, t) = \frac{\epsilon_0}{2} \left(\frac{\partial \mathbf{A}(\mathbf{x}, t)}{\partial t} \right)^2 + \frac{1}{2\mu_0} \mathbf{B}^2(\mathbf{x}, t) \quad (3)$$

is the kinetic photon term,

$$\mathcal{H}_{a\gamma}(\mathbf{x}, t) = \frac{1}{2m_a} \sum_s [iq_a \hbar \nabla \Psi_{a,s}^+(\mathbf{x}, t) \mathbf{A}(\mathbf{x}, t) \cdot \nabla \Psi_{a,s}(\mathbf{x}, t) - iq_a \hbar \nabla \Psi_{a,s}^+(\mathbf{x}, t) \cdot \mathbf{A}(\mathbf{x}, t) \Psi_{a,s}(\mathbf{x}, t) + q_a^2 \Psi_{a,s}^+(\mathbf{x}, t) \mathbf{A}^2(\mathbf{x}, t) \Psi_{a,s}(\mathbf{x}, t)] \quad (4)$$

is the matter-photon interaction term for particles of species a , and

$$\mathcal{H}_{ab}(\mathbf{x}, \mathbf{x}', t) = \sum_{s,s'} \frac{q_a q_b}{8\pi\epsilon_0 |\mathbf{x} - \mathbf{x}'|} \Psi_{a,s}^+(\mathbf{x}, t) \Psi_{b,s'}^+(\mathbf{x}', t) \times \Psi_{b,s'}(\mathbf{x}', t) \Psi_{a,s}(\mathbf{x}, t) \quad (5)$$

is the Coulomb interaction term between particle species a and b . All operator products are assumed to be normal ordered.

The mass dependence of $\mathcal{H}_{a\gamma}$ implies that matter-photon interactions are generically dominated by the electron-photon interaction terms (in the following we omit the electron labels: $m_e = m$, $\Psi_{e,s}(\mathbf{x}, t) = \Psi_s(\mathbf{x}, t)$),

$$\mathcal{H}_{e\gamma}(\mathbf{x}, t) = \frac{1}{2m} \sum_s [ie\hbar \nabla \Psi_s^+(\mathbf{x}, t) \cdot \mathbf{A}(\mathbf{x}, t) \Psi_s(\mathbf{x}, t) - ie\hbar \Psi_s^+(\mathbf{x}, t) \mathbf{A}(\mathbf{x}, t) \cdot \nabla \Psi_s(\mathbf{x}, t) + e^2 \Psi_s^+(\mathbf{x}, t) \mathbf{A}^2(\mathbf{x}, t) \Psi_s(\mathbf{x}, t)]. \quad (6)$$

The quantization conditions on the electron fields $\Psi_s(\mathbf{x}, t)$ and photon fields $\mathbf{A}(\mathbf{x}, t)$, and the relation between the electron field operators and electronic states and wave functions are briefly reviewed in Appendix B.

The minimal coupling terms (6) dominate photon-matter interactions in the visible, UV and X-ray regime,

* rainer.dick@usask.ca

and depending on the material under study, they can also dominate in the infrared regime. Exceptions can occur in the infrared wavelength range due to molecular vibrations and rotations, and in the microwave regime where spin-flipping Pauli terms can dominate due to the unavailability of spin-preserving electronic transitions.

Practitioners of photonics or spectroscopy are generically not interested in the technical details of the derivations of the pertinent quantum mechanical formulae for each particular kind of transition, while on the other hand there is no concise overview available of the pertinent formulae that covers all twelve types of optical transitions. The purpose of the present paper is therefore to provide such an overview as a resource for easy reference and for easy comparison of the formulae that apply to the different situations.

Indeed, the corresponding photon emission or absorption rates for transitions between discrete electronic energy levels are standard textbook examples, and photon absorption rates due to ionization are often reported through the Golden Rule. Furthermore, numerous applications of photon emission rates and absorption cross sections can be found in atomic, molecular and optical physics and throughout the spectroscopic literature, see e.g. [6] and references there. The unpolarized equations for photon absorption and emission due to transitions between discrete electronic states have also been compiled already by Hilborn [7], and the photon scattering cross section (including the Thomson term) due to transitions between discrete electron states is reported e.g. in [2, 5]. However, the corresponding equations for interband or intraband transitions in materials have never been discussed in a concise review, nor have all twelve cases of optical transitions been summarized in a single reference before.

Expressions in terms of densities of states in the energy scale are popular to describe transition rates and cross sections involving continuous electronic states in the material. However, this requires labeling of the continuous states in the form $|E, \nu\rangle$ with discrete degeneracy indices ν . This is in principle always possible through harmonic analysis, but is practical only if the particles are moving in a radially symmetric potential, when angular momentum quantum numbers $\nu = \{\ell, m_\ell\}$ provide discrete degeneracy indices on the constant energy surfaces $E(k_e) = E$. Formulations in terms of densities of states in the energy scale are therefore useful for the calculation of ionization rates in atomic physics. However, another practically important case of optical transitions involving continuous electron states concerns transitions from or into energy bands in materials, and in these cases we should formulate transition rates and cross sections in terms of Bloch energy eigenstates $|n, \mathbf{k}_e\rangle$. We will therefore provide equations in both formalisms.

All equations are given in dipole approximation, which is suitable up into the soft X-ray regime $E_\gamma \lesssim 1$ keV, $\lambda \gtrsim 1$ nm, and most results are displayed in “length form”, i.e. in terms of matrix elements of the position operator

\mathbf{x} ,

$$\langle f|\mathbf{x}|i\rangle = \int d^3\mathbf{x} \psi_f^+(\mathbf{x})\mathbf{x}\psi_i(\mathbf{x}). \quad (7)$$

Here we use upright notation for the quantum mechanical position operator \mathbf{x} or the momentum operator \mathbf{p} and standard italics notation for the corresponding classical vectors \mathbf{x} or \mathbf{p} . We also use upright notation for $i = \sqrt{-1}$ to distinguish it from labels for initial states $|i\rangle$. The initial and final wave functions $\psi_i(\mathbf{x})$ and $\psi_f(\mathbf{x})$ refer to energy eigenfunctions with corresponding eigenvalues E_i and E_f of H . At the level of the spectroscopic formulae compiled in this overview, the wave functions and energy eigenvalues refer to single nonrelativistic electrons moving in a potential $V(\mathbf{x})$, such that the first-quantized Hamiltonian is

$$H = \frac{\mathbf{p}^2}{2m} + V(\mathbf{x}). \quad (8)$$

The mass $m \equiv m_e = 511$ keV is the electron mass, because in many-electron atoms, in molecules, or in solid materials, the photons will couple to fundamental electrons through minimal coupling [8]. The emergence of effective single-electron Hamiltonians of the form (8) in many-electron systems from the quantum optics Hamiltonian (1) is briefly outlined in Appendix B.

Translation from the length form (7) into the “velocity form” in terms of matrix elements $\langle f|\mathbf{p}|i\rangle$ of the momentum operator \mathbf{p} proceeds through

$$\langle f|\mathbf{x}|i\rangle = \frac{\langle f|\mathbf{p}|i\rangle}{im\omega_{fi}}, \quad (9)$$

with the transition frequency

$$\omega_{fi} = -\omega_{if} = \frac{E_f - E_i}{\hbar}. \quad (10)$$

The transition rates in terms of the length form or the equivalent velocity form use the assumption that the electron states involved with photon emission, absorption or scattering are described through eigenstates of Hamiltonians of the form (8). The electron-photon coupling term (6) implies $\mathbf{p} \rightarrow \mathbf{p} + e\mathbf{A}(\mathbf{x}, t)$ in (8) and yields the leading-order electron-photon coupling terms $e[\mathbf{p} \cdot \mathbf{A}(\mathbf{x}, t) + \mathbf{A}(\mathbf{x}, t) \cdot \mathbf{p}]/2m$. This yields transition rates in velocity form in the first place. However, use of the length form is much more common and therefore this convention is also adopted here. All the length-form results listed below can be transformed back into the corresponding velocity forms through the substitution (9).

To keep the presentation as concise and useful as possible, technical remarks are kept to a minimum. However, details from the derivations of the formulae are included if they help to understand the structure and physical interpretations of the formulae. We denote initial and final electron states with $|i\rangle$ and $|f\rangle$, respectively. The letters i and f serve as placeholders for complete sets of quantum numbers for the electron states. We also indicate

the presence of a photon with γ , e.g. $|f, \gamma\rangle$ if there is also a photon in the final state. The letter γ serves as a placeholder for photon momentum $\hbar\mathbf{k}$ and polarization vector $\boldsymbol{\epsilon}_\gamma$.

The formulae for photon emission are listed in Sec. II, for photon absorption in Sec. III, and for photon scattering in Sec. IV. Within each Section, the different cases for the transitions $|i\rangle \rightarrow |f\rangle$ corresponding to discrete \rightarrow discrete, discrete \rightarrow continuous, continuous \rightarrow discrete and continuous \rightarrow continuous are organized in subsections, thus generating a catalogue and quasi-tabular overview of the pertinent formulae. Brief discussions of common labelings for continuous states, and of the quantum fields of quantum optics, are provided in Appendices A and B, respectively. Recoil effects are briefly discussed in Appendix C, and Appendix D contains a brief discussion of radiative electron-hole recombination in materials.

In keeping with the user-oriented spirit of this paper, a few formulations will be redundant between different subsections to ensure that a reader who is primarily interested e.g. in emission from decay of an acceptor state (i.e. emission due to a discrete \rightarrow continuous electronic transition) can directly jump to subsection IIB for the basic emission rates without having to consult the other subsections.

With respect to some special notations used in this paper, V without any argument denotes the volume of the Wigner-Seitz cell in a lattice, whereas the function $V(\mathbf{x})$ denotes a potential. The symbol \mathcal{V} without argument denotes the spatial volume factor in Fermi's trick $\delta^2(\mathbf{k}) \rightarrow \delta(\mathbf{k})\mathcal{V}/8\pi^3$ which also appears in the corresponding elementary volume unit in \mathbf{k} -space, $\Delta^3\mathbf{k} = 8\pi^3/\mathcal{V}$. In a crystal, we express this volume also as a sum of $N_{\mathbf{R}}$ Wigner-Seitz cells, $\mathcal{V} = N_{\mathbf{R}}V$. In Appendix B, the symbol $\mathcal{V}_e(\mathbf{x})$ denotes a potential operator in terms of quantized fields.

We use $\varrho_V(E)$ as the density of quantum states in the energy scale (e.g. in units of eV^{-1}) in a volume V , such that

$$N_{[E_1, E_2]}(V) = \int_{E_1}^{E_2} dE \varrho_V(E) \quad (11)$$

is the number of quantum states with energies in the range $E_1 \leq E \leq E_2$ in the volume V . The density of states $\varrho_V(E)$ is related to the local density of states $\varrho(E, \mathbf{x})$ (e.g. in units of $\text{eV}^{-1}\text{nm}^{-3}$) through volume integration,

$$\varrho_V(E) = \int_V d^3\mathbf{x} \varrho(E, \mathbf{x}). \quad (12)$$

Another manifestation $\tilde{\varrho}(E, \nu)$ of the density of states arises from contributions of the continuous parts C of the spectrum to completeness relations,

$$1 = \sum_{j, \nu} |E_j, \nu\rangle \langle E_j, \nu| + \sum_{\nu} \int_C dE |E, \nu\rangle \tilde{\varrho}(E, \nu) \langle E, \nu|. \quad (13)$$

Here E_j enumerates the discrete energy eigenvalues and ν is the set of degeneracy indices. The normalization and dimensions of the measure factors $\tilde{\varrho}(E, \nu)$ depend on the normalization and dimensions of the continuous energy eigenstates $|E, \nu\rangle$. The local density of states is given by the measure factors $\tilde{\varrho}(E, \nu)$ and the energy eigenfunctions through

$$\varrho(E, \mathbf{x}) = \sum_{j, \nu} |\langle \mathbf{x} | E_j, \nu \rangle|^2 \delta(E - E_j) + \sum_{\nu} |\langle \mathbf{x} | E, \nu \rangle|^2 \tilde{\varrho}(E, \nu), \quad (14)$$

see Appendix A for examples. Densities of states $\tilde{\varrho}(E, \nu)$ appear in transition rates involving electron states $|E, \nu\rangle$ in the continuous part of the spectrum. Densities of states $\varrho_V(E)$ occur in equations for transition rates involving initial or final states in an energy band, and V is the volume of the Wigner-Seitz cell in these cases.

II. PHOTON EMISSION $|i\rangle \rightarrow |f, \gamma\rangle$

Besides momentum $\hbar\mathbf{k}$, the polarization $\boldsymbol{\epsilon}$ is another basic property of photons. Polarization corresponds to a normalized vector, $\boldsymbol{\epsilon}^2 = 1$, that is perpendicular to the photon wave vector, $\boldsymbol{\epsilon} \cdot \mathbf{k} = 0$. As such, polarization can be expressed for every wave vector \mathbf{k} as a linear combination of a two-dimensional orthonormal basis that spans the plane perpendicular to \mathbf{k} , $\boldsymbol{\epsilon} = \sum_{\gamma} c_{\gamma} \boldsymbol{\epsilon}_{\gamma}(\mathbf{k})$, $\sum_{\gamma} |c_{\gamma}|^2 = 1$. Both Cartesian bases $\{\boldsymbol{\epsilon}_1(\mathbf{k}), \boldsymbol{\epsilon}_2(\mathbf{k})\}$ and circularly polarized bases with vectors $\boldsymbol{\epsilon}_{\pm}(\mathbf{k}) = [\boldsymbol{\epsilon}_1(\mathbf{k}) \pm i\boldsymbol{\epsilon}_2(\mathbf{k})]/\sqrt{2}$ are commonly used. Either way, summation over the tensor products of the basis vectors generates a 3×3 matrix that projects every vector onto the plane orthogonal to the wave vector,

$$\sum_{\gamma} \boldsymbol{\epsilon}_{\gamma}(\mathbf{k}) \otimes \boldsymbol{\epsilon}_{\gamma}^{\dagger}(\mathbf{k}) = \mathbf{1} - \hat{\mathbf{k}} \otimes \hat{\mathbf{k}}^T. \quad (15)$$

Here $\hat{\mathbf{k}} = \mathbf{k}/|\mathbf{k}|$ is the unit wave vector in the direction of photon motion. We will denote the polarization vector of a photon with $\boldsymbol{\epsilon}_{\gamma}(\mathbf{k}) \equiv \boldsymbol{\epsilon}_{\gamma}$ in the following, i.e. without the explicit reminder that it depends on \mathbf{k} through the requirement of orthogonality.

Depending on instrumentation and available photon beams, the practically relevant observables for photon emission concern polarized differential emission rates $d\Gamma_{fi}/d\Omega$, unpolarized differential emission rates $d\tilde{\Gamma}_{fi}/d\Omega = \sum_{\boldsymbol{\epsilon}_{\gamma}} d\Gamma_{fi}/d\Omega$, and unpolarized total emission rates $\tilde{\Gamma}_{fi} = \int d\Omega d\tilde{\Gamma}_{fi}/d\Omega$ [9]. The basic equations for all these quantities follow simple translation rules in terms of substitutions and scalings of the basic dipole transition factor $|\langle f | \boldsymbol{\epsilon}_{\gamma}^{\dagger} \cdot \mathbf{x} | i \rangle|^2$:

Differential emission rates $d\Gamma_{fi}/d\Omega$ for photons with polarization $\boldsymbol{\epsilon}_{\gamma}$ depend on $|\langle f | \boldsymbol{\epsilon}_{\gamma}^{\dagger} \cdot \mathbf{x} | i \rangle|^2$. For the translation into *unpolarized* differential emission rates $d\tilde{\Gamma}_{fi}/d\Omega$

we note that summation over photon polarizations for photons with momentum $\hbar\mathbf{k}$ yields

$$\sum_{\epsilon_\gamma} |\langle f | \epsilon_\gamma^+ \cdot \mathbf{x} | i \rangle|^2 = |\langle f | \mathbf{x} | i \rangle|^2 - |\langle f | \hat{\mathbf{k}} \cdot \mathbf{x} | i \rangle|^2. \quad (16)$$

For the translation of the polarized differential emission rate $d\Gamma_{fi}/d\Omega$ into the polarized total emission rate Γ_{fi} we note

$$\int d\Omega |\langle f | \epsilon_\gamma^+ \cdot \mathbf{x} | i \rangle|^2 = \frac{4\pi}{3} |\langle f | \mathbf{x} | i \rangle|^2. \quad (17)$$

The integration over angles has removed the dependence on the polarization. The equations for total unpolarized photon emission rates $\tilde{\Gamma}_{fi} = \sum_{\epsilon_\gamma} \int d\Omega d\Gamma_{fi}/d\Omega$ therefore satisfy $\tilde{\Gamma}_{fi} = 2\Gamma_{fi}$ and follow from the equations for $d\Gamma_{fi}/d\Omega$ through the substitution

$$|\langle f | \epsilon_\gamma^+ \cdot \mathbf{x} | i \rangle|^2 \rightarrow \frac{8\pi}{3} |\langle f | \mathbf{x} | i \rangle|^2. \quad (18)$$

Eqs. (24,25) provide an example for the substitution rule.

Eq. (17) is a consequence of the fact that for any two real vectors $\boldsymbol{\epsilon}$ and \mathbf{d} the equations

$$\int d\Omega (\boldsymbol{\epsilon} \cdot \mathbf{d})^2 = \frac{4\pi}{3} \boldsymbol{\epsilon}^2 \mathbf{d}^2 \quad (19)$$

and

$$\int d\Omega \boldsymbol{\epsilon} \cdot \mathbf{d} = 0 \quad (20)$$

hold. The vector

$$\langle f | \mathbf{x} | i \rangle = \mathbf{d}_{fi}^{(1)} + i\mathbf{d}_{fi}^{(2)} \quad (21)$$

will generically be complex, and the polarization vector

$$\boldsymbol{\epsilon}_\gamma = \boldsymbol{\epsilon}_\gamma^{(1)} + i\boldsymbol{\epsilon}_\gamma^{(2)}, \quad (\boldsymbol{\epsilon}_\gamma^{(1)})^2 + (\boldsymbol{\epsilon}_\gamma^{(2)})^2 = 1, \quad (22)$$

can be complex if we choose a chiral polarization basis. However, we can express the integrand in (17) in terms of products of real vectors in the form

$$\begin{aligned} |\langle f | \epsilon_\gamma^+ \cdot \mathbf{x} | i \rangle|^2 &= 2(\boldsymbol{\epsilon}_\gamma^{(1)} \times \boldsymbol{\epsilon}_\gamma^{(2)}) \cdot (\mathbf{d}_{fi}^{(1)} \times \mathbf{d}_{fi}^{(2)}) \\ &+ \sum_{ij} (\boldsymbol{\epsilon}_\gamma^{(i)} \cdot \mathbf{d}_{fi}^{(j)})^2, \end{aligned} \quad (23)$$

and this shows that Eq. (17) arises as a consequence of Eqs. (19,20).

A. Emission rates for both $|i\rangle$ and $|f\rangle$ discrete

This case applies e.g. to spontaneous photon emission due to transitions $|i\rangle \rightarrow |f\rangle$, $E_i > E_f$, between bound states in atoms or molecules. The differential emission

rate for photons with polarization ϵ_γ into a solid angle $d\Omega$ in the direction $\hat{\mathbf{k}}$ is

$$\frac{d\Gamma_{fi}}{d\Omega} = \frac{\alpha_S}{2\pi c^2} \omega_{if}^3 |\langle f | \epsilon_\gamma^+ \cdot \mathbf{x} | i \rangle|^2, \quad (24)$$

where $\alpha_S = e^2/4\pi\epsilon_0\hbar c$ is the fine structure constant. The total unpolarized emission rate is the Einstein A coefficient for the transition $|i\rangle \rightarrow |f\rangle$,

$$A_{fi} \equiv \tilde{\Gamma}_{fi} = \frac{4\alpha_S}{3c^2} \omega_{if}^3 |\langle f | \mathbf{x} | i \rangle|^2, \quad (25)$$

see also [7], where the relations to Einstein's B coefficients are also reviewed.

The initial and final states will initially depend on the spin projections (magnetic quantum numbers) s_i and s_f of the electrons in the initial state $|i\rangle$ and the final state $|f\rangle$, respectively. If we are not explicitly interested in transitions between spin-polarized states, transition rates are calculated in general through averaging over initial spin projection and summation over final spin projection, e.g.

$$\frac{d\Gamma_{fi}}{d\Omega} = \frac{1}{2} \sum_{s_f=-1/2}^{1/2} \sum_{s_i=-1/2}^{1/2} \frac{d\Gamma_{fi}}{d\Omega}(s_f, s_i). \quad (26)$$

The leading order electron-photon couplings (6) used in this review do not induce spin flips and Eq. (26) reduces to

$$\frac{d\Gamma_{fi}}{d\Omega} = \frac{1}{2} \sum_{s=-1/2}^{1/2} \frac{d\Gamma_{fi}}{d\Omega}(s, s) \quad (27)$$

for transitions through the interaction terms in Eq. (6). Note that the terms *polarized* or *unpolarized* in this paper always refer to photon polarization. Otherwise, we will use the term *spin-polarized*. Transition rates can depend on spin orientation if there are spin-polarized energy bands in materials as a consequence of spin-orbit coupling, exchange interactions, or external magnetic fields. All the formulae reported in this paper apply to these cases if spin orientation is properly included with the quantum numbers of states, and if Eq. (27) is used to derive spin-averaged transition rates.

Unpolarized emission rates like $\tilde{\Gamma}_{fi}$ or the corresponding absorption rates are traditionally often expressed in terms of the oscillator strengths,

$$F_{fi} = \frac{2m}{3\hbar} \omega_{fi} |\langle f | \mathbf{x} | i \rangle|^2 = -\frac{2m}{3\hbar} \omega_{if} |\langle f | \mathbf{x} | i \rangle|^2, \quad (28)$$

see e.g. [3] (where the corresponding one-dimensional definition is introduced) or [5]. Here we use the less common designation of capital F for the oscillator strength to avoid confusion with the label f for the final state.

The oscillator strengths (28) are dimensionless if both electronic states are discrete. Otherwise, they have dimensions commensurate with the labeling of the continuous states and their contributions to the completeness relations (A4,A5). A nice feature of the oscillator

strengths for discrete initial states $|i\rangle$ is the existence of sum rules when summed over the final states $|f\rangle$, where the appropriate measure factors from (A4,A5) need to be included when summing over the continuous parts of the spectrum. We will report all emission rates, absorption cross sections, and scattering cross sections directly in terms of the dipole matrix elements for easier comparison of the cases with discrete and continuous initial states.

Atomic recoils do not change the forms of Eqs. (24,25) because they do not introduce additional factors in the final results for emission rates. They only shift the transition frequency ω_{if} by small amounts, see Appendix C and in particular Eq. (C10).

B. Emission rates for $|i\rangle$ discrete and $|f\rangle$ continuous

This situation applies e.g. to electron-hole recombination if the electron was stored in an acceptor atom and the hole occurred in a valence band. The hole in the otherwise full valence band must be treated as a fixed initial particle state with momentum $-\mathbf{k}_e$ according to the principles of scattering theory.

However, as a preparation for this, it is useful to first consider the case of a highly excited acceptor or donor state $|i\rangle$ with energy $E_i > E_n(\mathbf{k}_e)$, which overlaps or is even above a conduction band $E_n(\mathbf{k}_e)$.

Continuous electron states are often labeled either through a wave vector \mathbf{k}_e , $|\mathbf{k}_e\rangle$, or through continuous energy eigenvalues E and discrete degeneracy indices ν , $|E, \nu\rangle$, see Appendix A. Examples of transitions from a discrete energy level into the \mathbf{k}_e -dependent levels of a lower lying energy band are depicted in Fig. 1.

Transitions can occur into the whole energy band, i.e. into Bloch states with arbitrary wave vector \mathbf{k}_e , because the Bloch wave vectors are confined to the Brillouin zone $k_e \leq \pi/a$ and the Bloch wavelengths $\lambda_e \geq 2a$ imply that the plane wave factors vary slowly over the extent of atomic wave functions.

The appearance of the density of states $\tilde{q}(E, \nu)$ in the contributions from the continuous states to the completeness relations (13) informs the appearance of $\tilde{q}(E, \nu)$ in transition rates involving continuous states.

The differential emission rate for photons with polarization ϵ_γ and frequency $ck = \omega_{if}$ into a solid angle $d\Omega$ due to transitions from the discrete initial state $|i\rangle$ into states $|f\rangle = |E_f, \nu_f\rangle$ in an energy range $[E_f, E_f + dE_f]$ below E_i is

$$\frac{d\Gamma_{fi}}{d\Omega} = \frac{\alpha_S}{2\pi c^2} \omega_{if}^3 |\langle f | \epsilon_\gamma^+ \cdot \mathbf{x} | i \rangle|^2 \tilde{q}_f(E_f) dE_f. \quad (29)$$

Please note that $\tilde{q}_f(E_f) \equiv \tilde{q}(E_f, \nu_f)$ only provides the density of states $|E_f, \nu_f\rangle$ with fixed degeneracy indices ν_f , see Appendix A.

Eq. (29) must be summed over the degeneracy indices ν_f if we are interested in the differential emission rate

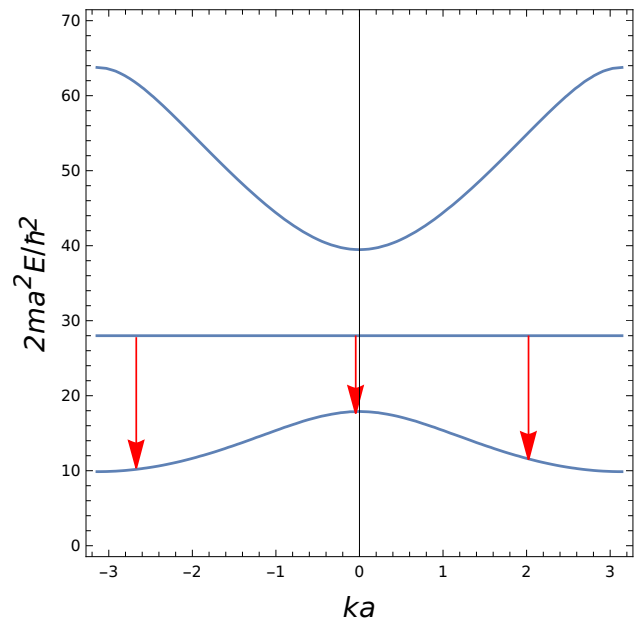


FIG. 1. Electronic transitions from a \mathbf{k}_e -independent discrete energy level into a lower lying energy band. The two bands depicted are the second and third energy bands in a Kronig-Penney model $V(x) = \mathcal{W} \sum_n \delta(x - na)$ with parameter $m\mathcal{W}a/\hbar^2 = -7$.

of all photons with frequency ck in a range $c[k, k + dk]$, which occur due to the decay of the state $|i\rangle$,

$$\frac{d\Gamma_i}{d\Omega dk} = \frac{\alpha_S}{2\pi} \hbar c^2 k^3 \sum_{\nu_f} |\langle f | \epsilon_\gamma^+ \cdot \mathbf{x} | i \rangle|^2 \tilde{q}_f(E_i - \hbar ck). \quad (30)$$

Continuous electron states in materials can be described as Bloch states with wave vectors \mathbf{k}_e and energy bands $E_n(\mathbf{k}_e)$,

$$|f\rangle = |n, \mathbf{k}_e\rangle = \sqrt{\frac{V}{8\pi^3}} \exp(i\mathbf{k}_e \cdot \mathbf{x}) |u_n(\mathbf{k}_e)\rangle. \quad (31)$$

Here V is the volume of the Wigner-Seitz cell and $|u_f\rangle = |u_n(\mathbf{k}_e)\rangle$ is the periodic Bloch factor of the final electron state.

The differential emission rate for transitions from an initial discrete state $|i\rangle$ into states with wave vector \mathbf{k}_e and energy $E_n(\mathbf{k}_e)$ in a volume $d^3\mathbf{k}_e$ in the Brillouin zone is

$$\frac{d\Gamma_{fi}}{d\Omega} = \frac{\alpha_S}{2\pi c^2} \omega_{if}^3 |\langle n, \mathbf{k}_e | \epsilon_\gamma^+ \cdot \mathbf{x} | i \rangle|^2 d^3\mathbf{k}_e. \quad (32)$$

To integrate this over the Brillouin zone, we use

$$d^3\mathbf{k}_e \rightarrow d^2\mathbf{k}_{e\parallel} \frac{dE_e}{|\partial E_n(\mathbf{k}_e)/\partial \mathbf{k}_e|}, \quad (33)$$

where $d^2\mathbf{k}_{e\parallel}$ is an integration measure on the constant energy surface $E_n(\mathbf{k}_e) = E_e$. Since $E_e = E_i - \hbar ck$, we have $|dE_e| = \hbar c dk$, and we get the analogue of Eq. (30)

for transition from the discrete state $|i\rangle$ into a lower-lying energy band $E_n(\mathbf{k}_e)$,

$$\frac{d\Gamma_i}{d\Omega dk} = \frac{\alpha_S}{2\pi} \hbar c^2 k^3 \times \int_{E_n(\mathbf{k}_e)=E_i-\hbar ck} d^2\mathbf{k}_{e\parallel} \frac{|\langle n, \mathbf{k}_e | \boldsymbol{\epsilon}_\gamma^+ \cdot \mathbf{x} | i \rangle|^2}{|\partial E_n(\mathbf{k}_e)/\partial \mathbf{k}_e|}. \quad (34)$$

The unpolarized differential emission rates into all directions from Eqs. (30) and (34) are

$$\frac{d\tilde{\Gamma}_i}{dk} = \frac{4\alpha_S}{3} \hbar c^2 k^3 \sum_{\nu_f} |\langle f | \mathbf{x} | i \rangle|^2 \tilde{\omega}_f(E_i - \hbar ck) \quad (35)$$

and

$$\frac{d\tilde{\Gamma}_i}{dk} = \frac{4\alpha_S}{3} \hbar c^2 k^3 \times \int_{E_n(\mathbf{k}_e)=E_i-\hbar ck} d^2\mathbf{k}_{e\parallel} \frac{|\langle n, \mathbf{k}_e | \mathbf{x} | i \rangle|^2}{|\partial E_n(\mathbf{k}_e)/\partial \mathbf{k}_e|}, \quad (36)$$

respectively.

Recoil of the emitting atom does not change the form of the equations (29-36) but can shift photon frequencies by small amounts, see Appendix C. Recoil is even more strongly suppressed through the embedding of the emitting acceptor atom in the crystal lattice, which amounts to $m_p \rightarrow \infty$ in Appendix C.

The case of a conduction band $E_n(\mathbf{k}_e)$ overlapping or below a highly excited acceptor or donor state $|i\rangle$ is not a common situation in solid state spectroscopy. Instead, we would rather encounter the case of a filled electron acceptor state $|i\rangle$ above a valence band $E_n(\mathbf{k}_e)$ with a hole in the electron state $|f\rangle = |n, \mathbf{k}_e\rangle$. In this case we have to consider the hole rather as a continuous initial state in the problem with a differential current density [10]

$$d\mathbf{J}_h(\mathbf{k}_e, \mathbf{x}) = -\psi_n^+(\mathbf{k}_e, \mathbf{x}) \frac{\hbar}{2im} \frac{\partial \psi_n(\mathbf{k}_e, \mathbf{x})}{\partial \mathbf{x}} d^3\mathbf{k}_e + \frac{\hbar}{2im} \frac{\partial \psi_n^+(\mathbf{k}_e, \mathbf{x})}{\partial \mathbf{x}} \psi_n(\mathbf{k}_e, \mathbf{x}) d^3\mathbf{k}_e. \quad (37)$$

Please note that the hole is still described by energy eigenvalues $E_n(\mathbf{k}_e)$ and the corresponding Bloch energy eigenfunctions, i.e. we are still dealing with a particle of mass m_e moving through the full periodic lattice potential without any parabolic band or effective mass approximation. For the evaluation of the electron recombination amplitude from the initially occupied acceptor state, the hole is also still described by the electronic annihilation operator $a_{n,s}(\mathbf{k}_e)$ that generates the vacancy in the valence band: In the hole picture, we go from a depleted Fermi ground state $a_{n,s}(\mathbf{k}_e)|\Omega\rangle$ (tensored with the occupied atomic acceptor state) to a full Fermi ground state $|\Omega\rangle$. However, after evaluation of all the operators, this still reduces to the differential transition rate (32).

The current density (37) depends on the position \mathbf{x} in the Wigner-Seitz cell due to the Bloch factors. Averaging over the Wigner-Seitz cell yields an analog of the

\mathbf{x} -independent current density of free particles,

$$\frac{d\mathbf{j}_h(\mathbf{k}_e)}{d^3\mathbf{k}_e} = \frac{1}{V} \int_V d^3\mathbf{x} \frac{d\mathbf{J}_h(\mathbf{k}_e, \mathbf{x})}{d^3\mathbf{k}_e}. \quad (38)$$

This can be used to divide the differential photon emission rate $d\Gamma_{fi}/(d\Omega d^3\mathbf{k}_e)$ from Eq. (32) by the norm $|d\mathbf{j}_h/d^3\mathbf{k}_e|$ of the differential current density, and integration over emission directions yields a hole capture cross section,

$$\sigma_{fi}(\mathbf{k}_e) = \frac{4\alpha_S}{3c^2} \omega_{if}^3 \frac{|\langle n, \mathbf{k}_e | \mathbf{x} | i \rangle|^2}{|d\mathbf{j}_h/d^3\mathbf{k}_e|}. \quad (39)$$

The photon emission rate due to hole capture from a hole current density $d\mathbf{j}_h(\mathbf{k}_e)/d^3\mathbf{k}_e$ with energy $E_f(\mathbf{k}_e)$ of the empty electron states is then the radiative hole capture rate,

$$\tilde{\Gamma}_{fi} = \int_{\mathcal{B}} d^3\mathbf{k}_e \sigma_{fi}(\mathbf{k}_e) |d\mathbf{j}_h(\mathbf{k}_e)/d^3\mathbf{k}_e|, \quad (40)$$

where the integration is over the Brillouin zone.

C. Emission rates for $|i\rangle$ continuous and $|f\rangle$ discrete

Photon emission from donor recombination with an electron from the conduction band or from annihilation of a core hole with a conduction electron are examples for these kinds of transitions. The initial Bloch state in the conduction band $E_n(\mathbf{k}_e)$ is $|i\rangle = |n, \mathbf{k}_e\rangle$.

Examples of transitions from an energy bandy into the \mathbf{k}_e -independent discrete energy level of an atom (e.g. from electron-donor recombination) are depicted in Fig. 2.

Transitions can occur from the whole energy band, i.e. from Bloch states with arbitrary wave vector \mathbf{k}_e , because the limit $\lambda_e \geq 2a$ on Bloch wavelengths implies that the plane wave factors vary slowly over the extent of atomic wave functions.

The process of radiative electron capture from the conduction band due to a discrete state below the conduction band is the mirror process to the radiative hole capture process (39). This yields an electron capture cross section for electrons with differential current density $d\mathbf{j}_e/d^3\mathbf{k}_e$,

$$\sigma_{fi} = \frac{4\alpha_S}{3c^2} \omega_{if}^3 \frac{|\langle f | \mathbf{x} | n, \mathbf{k}_e \rangle|^2}{|d\mathbf{j}_e/d^3\mathbf{k}_e|}, \quad (41)$$

and a corresponding photon emission rate from a differential electron current density $d\mathbf{j}_e/d^3\mathbf{k}_e$,

$$\tilde{\Gamma}_{fi} = \int d^3\mathbf{k}_e \sigma_{fi}(\mathbf{k}_e) |d\mathbf{j}_e(\mathbf{k}_e)/d^3\mathbf{k}_e|. \quad (42)$$

The observations from Appendix C about possible shifts in ω_{if} from atomic recoil apply here as well, with the note of additional suppression of recoil effects through embedding of the donor atom in the crystal lattice.

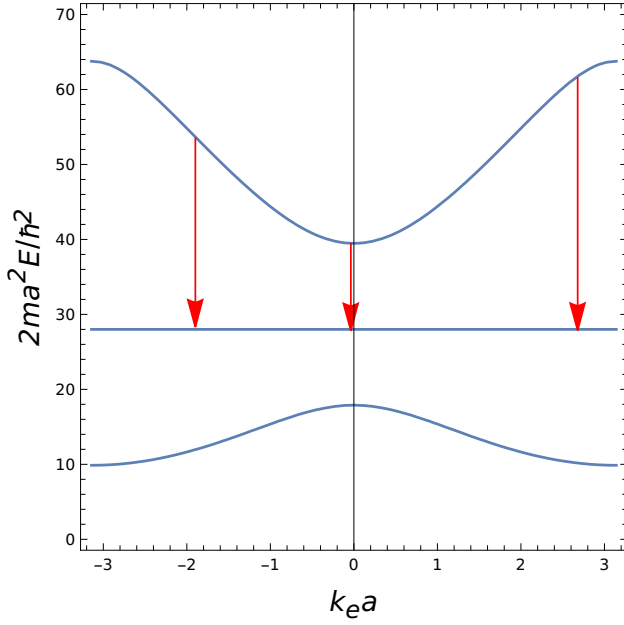


FIG. 2. Electronic transitions from an energy band into the \mathbf{k}_e -independent discrete energy level of an atom. The two bands depicted are the second and third energy bands in a Kronig-Penney model $V(x) = \mathcal{W} \sum_n \delta(x - na)$ with parameter $m\mathcal{W}a/\hbar^2 = -7$.

D. Emission rates for both $|i\rangle$ and $|f\rangle$ continuous

Photon processes involving both continuous initial and continuous final electronic states are very different from processes where at least one of the states is discrete. The presence of at least one discrete state usually requires presence of a participating atom or molecule, and while the atomic or molecular recoils balance momentum conservation in these processes, their impact on the transition rates is limited to a small shift in photon energies, see Appendix C. This is why we can effectively treat processes involving discrete electronic states as occurring due to interaction with a fixed atom or molecule and the corresponding scattering matrices then only involve energy conserving δ -functions but no momentum conserving δ -functions.

Continuous to continuous transitions, on the other hand, require interband transitions and the momentum conserving δ functions now track changes in electron momentum instead of atomic recoils. Since the wavelength of emitted (or absorbed) photons is much larger than typical lattice constants, momentum conservation for photon emission and absorption without phonon assistance leads to direct interband transitions relative to the size of the Brillouin zone. This is a consequence of the fact that energy bands do not change much on momentum scales which are very small relative to the size of the Brillouin zone. Energy conservation $\hbar c k = E_i(\mathbf{k}_{e,i}) - E_f(\mathbf{k}_{e,f})$

therefore simplifies due to

$$\begin{aligned} E_f(\mathbf{k}_{e,f}) &= E_f(\mathbf{k}_{e,i} - \mathbf{k}) \simeq E_f(\mathbf{k}_{e,i}) - \mathbf{k} \cdot \frac{\partial}{\partial \mathbf{k}_{e,i}} E_f(\mathbf{k}_{e,i}) \\ &\simeq E_f(\mathbf{k}_{e,i}), \end{aligned} \quad (43)$$

i.e. the energy of the emitted photon effectively corresponds to the energy difference between energy bands at the same point in the Brillouin zone.

Here we discuss the case of emission due to transition between conduction electron states, i.e. an electron in a higher conduction band jumps through photon emission into a lower conduction band, see Fig. 3 for a schematic.

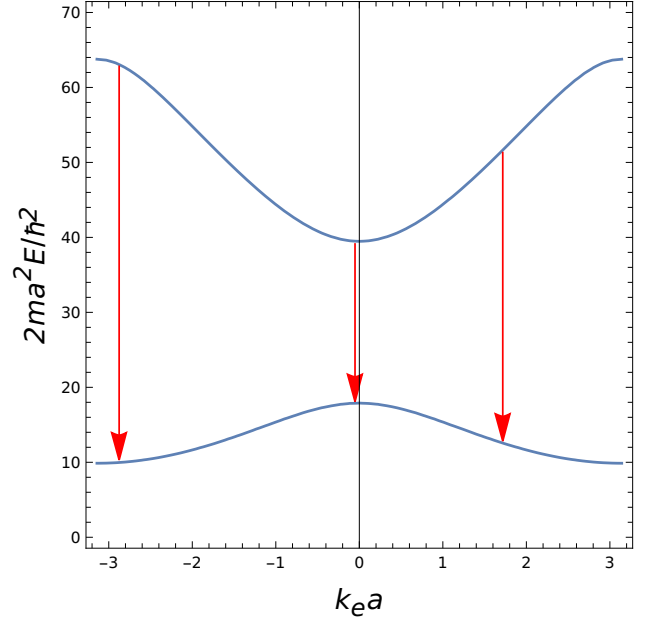


FIG. 3. Electronic transitions between the third and second energy band in a Kronig-Penney model $V(x) = \mathcal{W} \sum_n \delta(x - na)$ with parameter $m\mathcal{W}a/\hbar^2 = -7$.

The initial and final states are Bloch energy eigenstates with energy band indices n and electron wave vectors \mathbf{k}_e ,

$$\begin{aligned} \langle \mathbf{x} | i \rangle &= \langle \mathbf{x} | n_i, \mathbf{k}_{e,i} \rangle = \psi_{n_i}(\mathbf{k}_{e,i}, \mathbf{x}) \\ &= \sqrt{\frac{V}{8\pi^3}} \exp(i\mathbf{k}_{e,i} \cdot \mathbf{x}) u_{n_i}(\mathbf{k}_{e,i}, \mathbf{x}), \end{aligned} \quad (44)$$

$|f\rangle = |n_f, \mathbf{k}_{e,f}\rangle$. The orthogonality relation

$$\langle n, \mathbf{k}_e | n', \mathbf{k}'_e \rangle = \delta_{n,n'} \delta(\mathbf{k}_e - \mathbf{k}'_e) \quad (45)$$

of the Bloch states implies orthonormalization in the Wigner-Seitz cell for the Bloch factors with the same wave vector,

$$\begin{aligned} \langle u_n(\mathbf{k}_e) | u_{n'}(\mathbf{k}_e) \rangle_V &= \int_V d^3x u_n^\dagger(\mathbf{k}_e, \mathbf{x}) u_{n'}(\mathbf{k}_e, \mathbf{x}) \\ &= \delta_{n,n'}, \end{aligned} \quad (46)$$

where the integration is over the Wigner-Seitz cell.

The differential photon emission rate in the direction of photon momentum $\hat{\mathbf{k}}$ is

$$\begin{aligned} \frac{d\Gamma_{fi}}{d\Omega} &= \frac{\alpha_S}{2\pi c^2} \omega_{if}^3 |\langle f | \boldsymbol{\epsilon}_\gamma^+ \cdot \mathbf{x} | i \rangle_V|^2 \left(\frac{8\pi^3}{V} \right)^2 \\ &= \frac{\alpha_S}{2\pi c^2} \omega_{if}^3 |\langle u_f | \boldsymbol{\epsilon}_\gamma^+ \cdot \mathbf{x} | u_i \rangle_V|^2. \end{aligned} \quad (47)$$

The matrix element $\langle f | \boldsymbol{\epsilon}_\gamma^+ \cdot \mathbf{x} | i \rangle_V$ is integrated over the Wigner-Seitz cell, see (46).

The factor $(8\pi^3/V)^2$ appears in the first line of Eq. (47) because on the one hand, the \mathbf{k} -space volume of a fixed momentum state $|n, \mathbf{k}_e\rangle$ in a crystal of size $\mathcal{V} = N_{\mathbf{R}}V$ is $d^3\mathbf{k}_e = 8\pi^3/N_{\mathbf{R}}V$, where $N_{\mathbf{R}}$ is the number of lattice cells. On the other hand, summation over the locations \mathbf{R} of lattice cells yields

$$\sum_{\mathbf{R}} \exp[i(\mathbf{k}_{e,i} - \mathbf{k}_{e,f} - \mathbf{k}) \cdot \mathbf{R}] = \frac{8\pi^3}{V} \delta(\mathbf{k}_{e,i} - \mathbf{k}_{e,f} - \mathbf{k}). \quad (48)$$

This factor occurs in the calculation of the scattering matrix element for the photon emission. The differential photon emission rate from the lattice therefore incurs a factor

$$\begin{aligned} \left[\frac{8\pi^3}{V} \delta(\mathbf{k}_{e,i} - \mathbf{k}_{e,f} - \mathbf{k}) \right]^2 d^3\mathbf{k}_{e,i} &= \frac{8\pi^3}{V} \delta(\mathbf{k}_{e,i} - \mathbf{k}_{e,f} - \mathbf{k}) \\ &\quad \times N_{\mathbf{R}} \frac{8\pi^3}{N_{\mathbf{R}}V}. \end{aligned} \quad (49)$$

The momentum conserving δ -function is absorbed by integration over the momentum of the final electron state.

The corresponding unpolarized emission rate into all directions is

$$\tilde{\Gamma}_{fi} = \frac{4\alpha_S}{3c^2} \omega_{if}^3 |\langle u_f | \mathbf{x} | u_i \rangle_V|^2. \quad (50)$$

It should be emphasized that Eqs. (47,50) apply to transitions between conduction bands, but not to a conduction electron filling a valence band hole. Due to kinematic constraints, photon emission from electron-hole recombination between conduction and valence band states should be impacted by higher order processes like phonon assistance, emission of Auger electrons, trapping of particles, or two-photon emission. It is therefore outside of the scope of this review, see also Appendix D.

III. PHOTON ABSORPTION $|i, \gamma\rangle \rightarrow |f\rangle$

In the case of photon absorption, the differential absorption rate $d\mathcal{A}_{fi}/d^3\mathbf{k}$ for photons with momentum $\hbar\mathbf{k}$ is divided by the differential current density $|d\mathbf{j}_\gamma/d^3\mathbf{k}|$ of the incoming photons to yield a measure for the efficiency of photon absorption through a transition $|i, \gamma\rangle \rightarrow |f\rangle$. This yields the absorption cross section $\sigma_{fi} = (d\mathcal{A}_{fi}/d^3\mathbf{k})/|d\mathbf{j}_\gamma/d^3\mathbf{k}|$.

The absorption cross section

$$\sigma_{fi}(\boldsymbol{\epsilon}_\alpha) = [d\mathcal{A}_{fi}(\boldsymbol{\epsilon}_\alpha)/d^3\mathbf{k}]/|d\mathbf{j}_\gamma(\boldsymbol{\epsilon}_\alpha)/d^3\mathbf{k}| \quad (51)$$

for photons with polarization $\boldsymbol{\epsilon}_\alpha$ depends on $|\langle f | \boldsymbol{\epsilon}_\alpha \cdot \mathbf{x} | i \rangle|^2$ and therefore on angles between the vectors $\boldsymbol{\epsilon}_\alpha$ and $\langle f | \mathbf{x} | i \rangle$. Averaging over those angles yields

$$\frac{1}{4\pi} \int d\Omega |\langle f | \boldsymbol{\epsilon}_\gamma \cdot \mathbf{x} | i \rangle|^2 = \frac{1}{3} |\langle f | \mathbf{x} | i \rangle|^2, \quad (52)$$

thus removing the dependence on polarization, see also Eqs. (17) and (19-23).

On the other hand, normalization by the unpolarized photon current density $d\mathbf{j}_\gamma/d^3\mathbf{k} = \sum_\alpha d\mathbf{j}_\gamma(\boldsymbol{\epsilon}_\alpha)/d^3\mathbf{k}$ and $d\mathbf{j}_\gamma(\boldsymbol{\epsilon}_1)/d^3\mathbf{k} = d\mathbf{j}_\gamma(\boldsymbol{\epsilon}_2)/d^3\mathbf{k}$ for unpolarized currents implies that the unpolarized cross section is the average of the polarized cross sections,

$$\sigma_{fi} = \frac{1}{|d\mathbf{j}_\gamma/d^3\mathbf{k}|} \sum_{\alpha=1}^2 \frac{d\mathcal{A}_{fi}(\boldsymbol{\epsilon}_\alpha)}{d^3\mathbf{k}} = \frac{1}{2} \sum_{\alpha=1}^2 \sigma_{fi}(\boldsymbol{\epsilon}_\alpha). \quad (53)$$

Since angle averaging removes polarization dependence (52), the angle averaged absorption cross section

$$\bar{\sigma}_{fi} = \frac{1}{4\pi} \int d\Omega \sigma_{fi} \quad (54)$$

has the same value for polarized and unpolarized photons. Furthermore, Eq. (52) implies that $\bar{\sigma}_{fi}$ is gotten from σ_{fi} through the substitution

$$|\langle f | \boldsymbol{\epsilon}_\gamma \cdot \mathbf{x} | i \rangle|^2 \rightarrow \frac{1}{3} |\langle f | \mathbf{x} | i \rangle|^2. \quad (55)$$

An example is provided in Eqs. (57,58). Due to the simple substitution rule (55) we will only write down the polarized absorption cross sections σ_{fi} in other cases.

If we are interested in the absorption cross sections for all photons with frequency ω_{fi} due to absorption from the initial state $|i\rangle$, we need to sum the equations for the absorption cross sections σ_{fi} over the degeneracy indices ν_f of the final states,

$$\sigma_i \Big|_{ck=\omega_{fi}} = \sum_{\nu_f} \sigma_{fi}. \quad (56)$$

A. Absorption cross sections for both $|i\rangle$ and $|f\rangle$ discrete

The absorption cross section for photons with polarization $\boldsymbol{\epsilon}_\gamma$ and momentum $\hbar\mathbf{k}$ is

$$\sigma_{fi} = 4\pi^2 \alpha_S \omega_{fi} |\langle f | \boldsymbol{\epsilon}_\gamma \cdot \mathbf{x} | i \rangle|^2 \delta(\omega_{fi} - ck). \quad (57)$$

The angle averaged absorption cross section for polarized or unpolarized photons follows immediately from (52),

$$\bar{\sigma}_{fi} = \frac{4\pi^2}{3} \alpha_S \omega_{fi} |\langle f | \mathbf{x} | i \rangle|^2 \delta(\omega_{fi} - ck). \quad (58)$$

Eqs. (57,58) follow in the displayed forms directly from the scattering matrix in first order time-dependent perturbation theory. However, closer examination of the

transition rates through inclusion of the reduction of the initial state in a coupled set of rate equations [3, 11] or through the resolvent operator [1, 12] replaces the energy conserving δ function in Eqs. (57,58) with a Lorentz profile $\Delta_\Gamma(\omega_{fi} - ck)$ of width 2Γ ,

$$\delta(\omega_{fi} - ck) \rightarrow \Delta_\Gamma(\omega_{fi} - ck) = \frac{1}{\pi} \frac{\Gamma}{(\omega_{fi} - ck)^2 + \Gamma^2}. \quad (59)$$

We have to be careful, however, to note that the direct substitution (59) only works as an approximation for narrow spectral lines, $\Gamma \ll \omega_{fi}$, when we are always at or near resonance. Otherwise an additional factor ω_{fi}/ck would appear in Eqs. (57,58) because there would be the factor ω_{fi}^2 arising from Eq. (9), $\langle f|\mathbf{p}|i\rangle = im\omega_{fi}\langle f|\mathbf{x}|i\rangle$, and there would be a factor $1/ck$ arising from a factor $1/\sqrt{ck}$ in the mode expansion of the vector potential. Furthermore, wide lines may be caused by other line broadening effects besides lifetime broadening and a Lorentzian profile may not be appropriate anymore.

B. Absorption cross sections for $|i\rangle$ discrete and $|f\rangle$ continuous

This case applies e.g. to ionization of an atom or of a donor in a semiconductor, see Fig. 4 for a schematic.

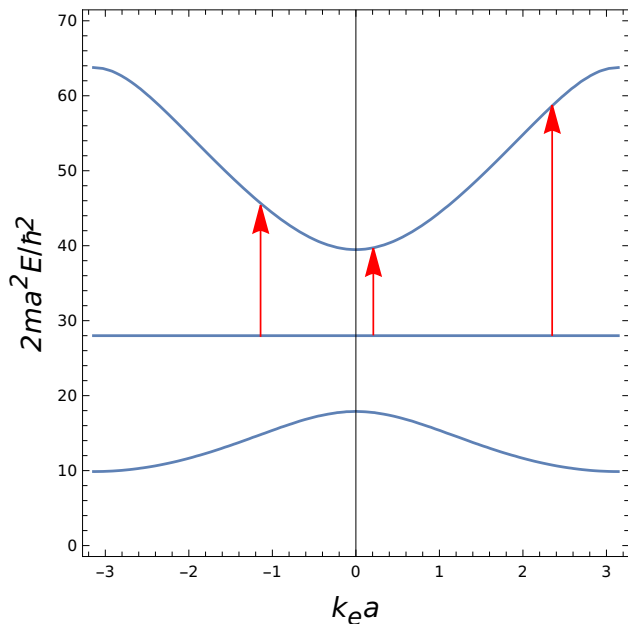


FIG. 4. Electronic transitions from a \mathbf{k}_e -independent discrete donor level into a higher energy band. The two bands depicted are the second and third energy bands in a Kronig-Penney $V(x) = \mathcal{W} \sum_n \delta(x - na)$ with parameter $m\mathcal{W}a/\hbar^2 = -7$.

Transitions can occur into the whole energy band, i.e. into Bloch states with arbitrary wave vector \mathbf{k}_e , because the limit $\lambda_e \geq 2a$ on Bloch wavelengths implies that the plane wave factors vary slowly over the extent of atomic wave functions.

The polarized absorption cross section for transition into states $|f\rangle = |E_f, \nu_f\rangle$ in the energy range $[E_f, E_f + dE_f]$ and with discrete degeneracy indices ν_f is

$$\sigma_{fi} = 4\pi^2 \alpha_S \hbar ck [\tilde{\varrho}_f(E_f) |\langle f|\boldsymbol{\epsilon}_\gamma \cdot \mathbf{x}|i\rangle|^2]_{E_f=E_i+\hbar ck}. \quad (60)$$

On the other hand, if $|i\rangle$ is a discrete donor state and $|f\rangle = |n, \mathbf{k}_e\rangle$ are states in the conduction band $E_n(\mathbf{k}_e)$, the differential absorption cross section for polarized photons of frequency ck from occupied donor states $|i\rangle$ due to electron excitation into the conduction band is

$$d\sigma_{fi} = 4\pi^2 \alpha_S \omega_{fi} |\langle n, \mathbf{k}_e|\boldsymbol{\epsilon}_\gamma \cdot \mathbf{x}|i\rangle|^2 \delta(\omega_{fi} - ck) d^3 \mathbf{k}_e. \quad (61)$$

The total contribution from the conduction band $E_n(\mathbf{k}_e)$ to the absorption cross section for polarized photons of frequency ck is

$$\begin{aligned} \sigma_{ni} &= 4\pi^2 \alpha_S \hbar ck \\ &\times \int_{\mathcal{B}} d^3 \mathbf{k}_e |\langle n, \mathbf{k}_e|\boldsymbol{\epsilon}_\gamma \cdot \mathbf{x}|i\rangle|^2 \delta(E_n(\mathbf{k}_e) - E_i - \hbar ck) \\ &= 4\pi^2 \alpha_S \hbar ck \\ &\times \int_{E_n(\mathbf{k}_e)=E_i+\hbar ck} d^2 \mathbf{k}_{e\parallel} \frac{|\langle n, \mathbf{k}_e|\boldsymbol{\epsilon}_\gamma \cdot \mathbf{x}|i\rangle|^2}{|\partial E_n(\mathbf{k}_e)/\partial \mathbf{k}_e|}. \end{aligned} \quad (62)$$

Here $d^2 \mathbf{k}_{e\parallel}$ is an integration measure along the constant energy surface $E_n(\mathbf{k}_e) = E_i + \hbar ck$ in the Brillouin zone \mathcal{B} .

If the matrix element $|\langle n, \mathbf{k}_e|\boldsymbol{\epsilon}_\gamma \cdot \mathbf{x}|i\rangle|^2$ is approximately constant over the constant energy surface, we find an equation very similar to (60),

$$\begin{aligned} \sigma_{ni} &= 4\pi^2 \alpha_S \hbar ck \\ &\times [\varrho_{n,V}(E_f) |\langle u_n(\mathbf{k}_e)|\boldsymbol{\epsilon}_\gamma \cdot \mathbf{x}|i\rangle|^2]_{E_f=E_i+\hbar ck}, \end{aligned} \quad (63)$$

with the density of states $\varrho_{n,V}(E)$ in the energy band $E_n(\mathbf{k}_e)$,

$$\varrho_{n,V}(E) = \frac{V}{8\pi^3} \int_{E_n(\mathbf{k}_e)=E} \frac{d^2 \mathbf{k}_{e\parallel}}{|\partial E_n(\mathbf{k}_e)/\partial \mathbf{k}_e|}. \quad (64)$$

Here we used that the discrete initial state $|i\rangle$ should be localized within a Wigner-Seitz cell and therefore $\exp(i\mathbf{k}_e \cdot \mathbf{x}) \simeq 1$ in the matrix element.

Intuitively, the assumption of approximately constant factor $|\langle u_n(\mathbf{k}_e)|\boldsymbol{\epsilon}_\gamma \cdot \mathbf{x}|i\rangle|^2$ across the constant energy surface $E_n(\mathbf{k}_e) = E_i + \hbar ck$ could be justified if that energy surface is small compared to the typical area $4\pi^2/V^{2/3}$ of the Brillouin zone. The integral in (34) then spans a relatively small surface area in the Brillouin zone such that the Bloch factor does not vary a lot with \mathbf{k}_e .

For the interpretation of Eq. (64), we note that the local number of spin-polarized electron states in the phase space volume $d^3 \mathbf{x} d^3 \mathbf{k}_e$ and in the energy band $E_n(\mathbf{k}_e)$ is

$$\begin{aligned} dN_n(\mathbf{k}_e, \mathbf{x}) &= |\langle \mathbf{x}|n, \mathbf{k}_e\rangle|^2 d^3 \mathbf{x} d^3 \mathbf{k}_e \\ &= \frac{V}{8\pi^3} |\langle \mathbf{x}|u_n(\mathbf{k}_e)\rangle|^2 d^3 \mathbf{x} d^3 \mathbf{k}_e. \end{aligned} \quad (65)$$

The density $\varrho_{n,V}(E)$ is therefore the contribution from the energy band $E_n(\mathbf{k}_e)$ to the density of spin-polarized electron states in the energy scale and in the Wigner-Seitz cell, i.e.

$$N_{[E_1, E_2]}^{(n)} = \int_{E_1}^{E_2} dE \varrho_{n,V}(E) \quad (66)$$

is the contribution from the energy band $E_n(\mathbf{k}_e)$ to the number of spin-polarized electron states in the Wigner-Seitz cell and with energies $E_1 \leq E \leq E_2$.

Eq. (60) is exact (within the limits of first-order perturbation theory and dipole approximation) since we assumed fixed discrete degeneracy indices ν_f in the final continuous state, whereas here we have continuous degeneracy indices $\mathbf{k}_{e\parallel}$ tangential to the surface of constant energy, and we integrated over those degeneracy indices while ignoring the factor $|\langle n, \mathbf{k}_e | \boldsymbol{\epsilon}_\gamma \cdot \mathbf{x} | i \rangle|^2$. The density of states $\tilde{\varrho}_f(E_f)$ in the exact equation (60) is therefore a density of states for fixed discrete degeneracy indices ν_f , whereas the density of states $\varrho_{n,V}(E_f)$ in the approximate equation (63) is integrated over degeneracies. On the other hand, summation over the discrete degeneracy indices in (60) would yield the same result as the integration in (62).

C. Absorption cross sections for $|i\rangle$ continuous and $|f\rangle$ discrete

This applies e.g. to ionization of an acceptor due to acceptance of a valence band electron, see Fig. 5 for a schematic.

Transitions can occur from the whole energy band, i.e. from initial Bloch states with arbitrary wave vector \mathbf{k}_e , because the limit $\lambda_e \geq 2a$ on Bloch wavelengths implies that the plane wave factors vary slowly over the extent of atomic wave functions.

The polarized absorption cross section for transition from initial states $|i\rangle = |E_i, \nu_i\rangle$ in the energy range $[E_i, E_i + dE_i]$ is

$$\sigma_{fi} = 4\pi^2 \alpha_S \hbar c k \left[\tilde{\varrho}_i(E_i) |\langle f | \boldsymbol{\epsilon}_\gamma \cdot \mathbf{x} | i \rangle|^2 \right]_{E_f = E_i + \hbar c k}. \quad (67)$$

Eq. (67) assumes discrete degeneracy indices ν_i and $\tilde{\varrho}_i(E_i) \equiv \tilde{\varrho}(E_i, \nu_i)$. On the other hand, if the initial state is a Bloch state $|i\rangle = |n, \mathbf{k}_e\rangle$ in an energy band $E_n(\mathbf{k}_e)$, the differential absorption cross section from transitions into the discrete acceptor state $|f\rangle$ is

$$d\sigma_{fi} = 4\pi^2 \alpha_S c k |\langle f | \boldsymbol{\epsilon}_\gamma \cdot \mathbf{x} | n, \mathbf{k}_e \rangle|^2 \delta(\omega_{fi} - ck) d^3 \mathbf{k}_e. \quad (68)$$

The contribution from the whole energy band to the absorption cross section is therefore

$$\sigma_{fn} = 4\pi^2 \alpha_S \hbar c k \times \int_{E_n(\mathbf{k}_e) = E_i} d^2 \mathbf{k}_{e\parallel} \frac{|\langle f | \boldsymbol{\epsilon}_\gamma \cdot \mathbf{x} | n, \mathbf{k}_e \rangle|^2}{|\partial E_n(\mathbf{k}_e) / \partial \mathbf{k}_e|}. \quad (69)$$

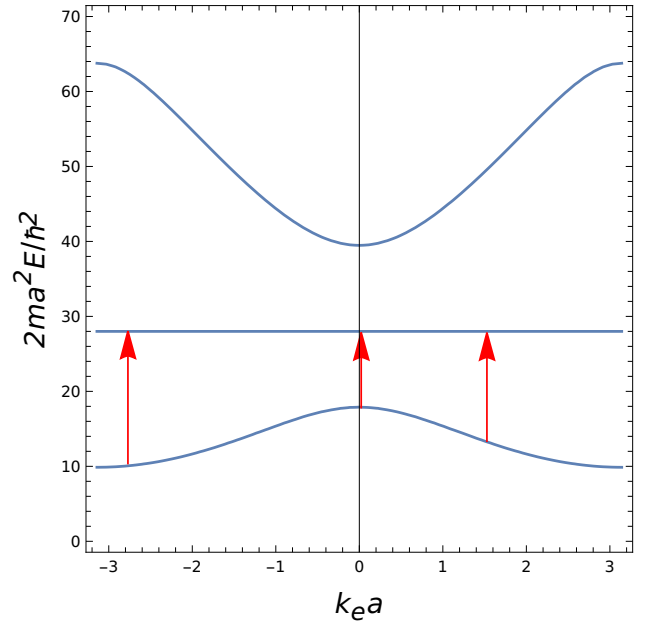


FIG. 5. Electronic transitions from an energy band into a \mathbf{k}_e -independent discrete acceptor level. The two bands depicted are the second and third energy bands in a Kronig-Penney $V(x) = \mathcal{W} \sum_n \delta(x - na)$ with parameter $m\mathcal{W}a/\hbar^2 = -7$.

Just as in the previous subsection, the assumption of approximately constant matrix element across the constant energy surface yields an approximation that resembles Eq. (67),

$$\sigma_{fn} = 4\pi^2 \alpha_S \hbar c k \times [\varrho_{n,V}(E_i) |\langle f | \boldsymbol{\epsilon}_\gamma \cdot \mathbf{x} | u_n(\mathbf{k}_e) \rangle|^2]_{E_f = E_i + \hbar c k} \quad (70)$$

with the density of states (64).

Eq. (69) includes a sum over the continuous degeneracy indices corresponding to the integration measure $d^2 \mathbf{k}_{e\parallel}$ on the constant energy surface $E_n(\mathbf{k}_e) = E_i$. This corresponds to summation over the discrete degeneracy indices ν_i in Eq. (67).

D. Absorption cross sections for both $|i\rangle$ and $|f\rangle$ continuous

This applies to absorption due to interband transitions, see Fig. 6 for a schematic. The same remarks as in subsection II D concerning momentum conservation apply.

The contribution from the transition $|i\rangle = |n, \mathbf{k}_e\rangle \rightarrow |f\rangle = |n', \mathbf{k}_e\rangle$ to the absorption cross section for polarized photons of frequency ck is

$$\sigma_{fi} = 4\pi^2 \alpha_S c k \delta(\omega_{fi} - ck) |\langle u_f | \boldsymbol{\epsilon}_\gamma \cdot \mathbf{x} | u_i \rangle_V|^2, \quad (71)$$

where V is the volume of the Wigner-Seitz cell and $|u_i\rangle$ or $|u_f\rangle$ are the Bloch factors of the initial and final states, respectively, see Eq. (A1). The matrix element $\langle u_f | \boldsymbol{\epsilon}_\gamma \cdot \mathbf{x} | u_i \rangle_V$ is integrated over the Wigner-Seitz cell.

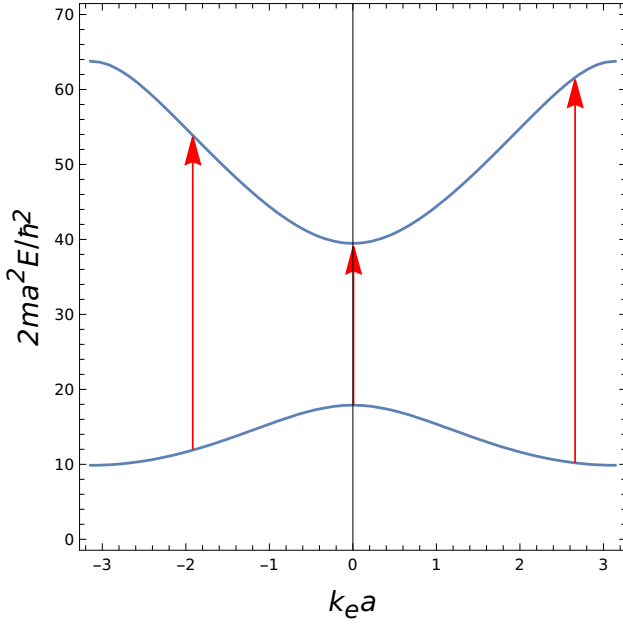


FIG. 6. Electronic transitions between the second and third energy band in a Kronig-Penney model $V(x) = \mathcal{W} \sum_n \delta(x - na)$ with parameter $m\mathcal{W}a/\hbar^2 = -7$.

The absorption cross section per lattice cell from the interband transition $E_n(\mathbf{k}_e) \rightarrow E_{n'}(\mathbf{k}_e)$ is

$$\begin{aligned} \sigma_{n'n} &= \frac{V}{8\pi^3} \int d^3 \mathbf{k}_e \sigma_{fi} \\ &= \frac{\alpha_S}{2\pi} \hbar c k V \int_{E_{n'}(\mathbf{k}_e) - E_n(\mathbf{k}_e) = \hbar c k} d^2 \mathbf{k}_{e\parallel} \\ &\quad \times \frac{|\langle u_{n'}(\mathbf{k}_e) | \boldsymbol{\epsilon}_\gamma \cdot \mathbf{x} | u_n(\mathbf{k}_e) \rangle_V|^2}{|\partial[E_{n'}(\mathbf{k}_e) - E_n(\mathbf{k}_e)]/\partial \mathbf{k}_e|}. \end{aligned} \quad (72)$$

Pulling the factor $|\langle u_{n'}(\mathbf{k}_e) | \boldsymbol{\epsilon}_\gamma \cdot \mathbf{x} | u_n(\mathbf{k}_e) \rangle_V|^2$ out of the integral under the assumption that it is approximately constant over the surface $E_{n'}(\mathbf{k}_e) - E_n(\mathbf{k}_e) = \hbar c k$ yields an equation which resembles Eqs. (60,67),

$$\begin{aligned} \sigma_{n'n} &= 4\pi^2 \alpha_S \hbar c k |\langle u_{n'}(\mathbf{k}_e) | \boldsymbol{\epsilon}_\gamma \cdot \mathbf{x} | u_n(\mathbf{k}_e) \rangle_V|^2 \\ &\quad \times \varrho_{n'n,V}(\hbar c k) \end{aligned} \quad (73)$$

with the joint density of states

$$\begin{aligned} \varrho_{n'n}(E) &= \frac{V}{8\pi^3} \int d^3 \mathbf{k}_e \delta(E_{n'}(\mathbf{k}_e) - E_n(\mathbf{k}_e) - E) \\ &= \frac{V}{8\pi^3} \int_{E_{n'}(\mathbf{k}_e) - E_n(\mathbf{k}_e) = E} d^2 \mathbf{k}_{e\parallel} \\ &\quad \times \frac{1}{|\partial[E_{n'}(\mathbf{k}_e) - E_n(\mathbf{k}_e)]/\partial \mathbf{k}_e|}. \end{aligned} \quad (74)$$

The reasoning that led to the interpretation of $\varrho_n(E)$ (64) implies that the joint density of states (74) yields the spin-polarized number $\varrho_{n'n,V}(E)dE$ of pairs of electron states in the Wigner-Seitz cell which are contributed by the energy bands $E_{n'}(\mathbf{k}_e)$ and $E_n(\mathbf{k}_e)$ and satisfy $E_{n'}(\mathbf{k}_e) - E_n(\mathbf{k}_e) \in [E, E + dE]$.

IV. PHOTON SCATTERING $|i, \gamma\rangle \rightarrow |f, \gamma'\rangle$

The differential scattering cross sections for photon scattering $|i; \boldsymbol{\epsilon}_\gamma, \mathbf{k}\rangle \rightarrow |f; \boldsymbol{\epsilon}'_{\gamma'}, \mathbf{k}'\rangle$ involve sums over intermediate electron states $|v\rangle$ in the form $\sum_v |v\rangle f(E_v) \langle v|$, where $f(E_v) = \hbar/(E_v - E_i - \hbar c k)$ or $f(E_v) = \hbar/(E_v - E_i + \hbar c k')$, respectively, in the two scattering terms that appear in the Kramers-Heisenberg formula, see Eq. (82) below. The sum over the intermediate states is just a shorthand notation for sums over discrete intermediate electron states $|d\rangle$ (e.g. donor or acceptor states) and continuous intermediate electron states, e.g. due to transition through intermediate states $|n, \mathbf{k}_e\rangle$ in energy bands $E_n(\mathbf{k}_e)$,

$$\begin{aligned} \sum_v |v\rangle f(E_v) \langle v| &\equiv \sum_d |d\rangle f(E_d) \langle d| \\ &\quad + \sum_n \int d^3 \mathbf{k}_e |n, \mathbf{k}_e\rangle f(E_n(\mathbf{k}_e)) \langle n, \mathbf{k}_e|. \end{aligned}$$

A. Differential scattering cross section for both $|i\rangle$ and $|f\rangle$ discrete

This case applies to scattering between initial and final bound atomic states, e.g. core states in lattice atoms or bound states of acceptor or donor atoms. A schematic involving resonantly enhanced scattering through intermediate energy band states is depicted in Fig. 7

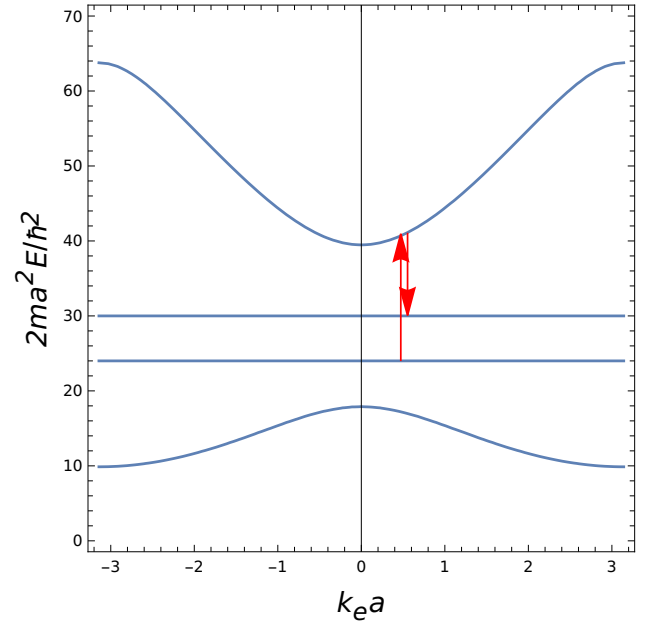


FIG. 7. Scattering between \mathbf{k}_e -independent discrete atomic energy levels. In this case the scattering is resonantly enhanced through an intermediate band state. The depicted bands correspond to the second and third energy band in a Kronig-Penney model $V(x) = \mathcal{W} \sum_n \delta(x - na)$ with parameter $m\mathcal{W}a/\hbar^2 = -7$.

Transitions can involve intermediate states in the whole energy band, i.e. intermediate Bloch states with arbitrary wave vector \mathbf{k}_e , because the limit $\lambda_e \geq 2a$ on Bloch wavelengths implies that the plane wave factors vary slowly over the extent of the atomic wave functions.

Minimal coupling $\mathbf{p} \rightarrow \mathbf{p} + e\mathbf{A}(\mathbf{x}, t)$ of photons into the Schrödinger equation yields the differential photon scattering cross section [13–15]

$$\begin{aligned} \frac{d\sigma}{d\Omega} &= \left(\frac{\alpha_S}{m^2 c}\right)^2 \frac{k'}{k} \\ &\times \left| m\hbar\delta_{fi}\boldsymbol{\epsilon}'_\gamma \cdot \boldsymbol{\epsilon}_\gamma - \sum_v \frac{\langle f|\boldsymbol{\epsilon}'_\gamma \cdot \mathbf{p}|v\rangle\langle v|\boldsymbol{\epsilon}_\gamma \cdot \mathbf{p}|i\rangle}{\omega_{vi} - ck - i\eta} \right. \\ &\left. - \sum_v \frac{\langle f|\boldsymbol{\epsilon}_\gamma \cdot \mathbf{p}|v\rangle\langle v|\boldsymbol{\epsilon}'_\gamma \cdot \mathbf{p}|i\rangle}{\omega_{vi} + ck' - i\eta} \right|_{\omega_{fi}=ck-ck'}^2. \end{aligned} \quad (75)$$

Here we use $\boldsymbol{\epsilon}'_\gamma \equiv \boldsymbol{\epsilon}^+(\mathbf{k}')$ for the polarization vector of the emitted photon while $\boldsymbol{\epsilon}_\gamma \equiv \boldsymbol{\epsilon}(\mathbf{k})$ is the polarization vector of the incident photon.

The differential scattering cross section with the matrix elements in length form is

$$\begin{aligned} \frac{d\sigma}{d\Omega} &= \left(\frac{\alpha_S}{c}\right)^2 \frac{k'}{k} \\ &\times \left| \frac{\hbar}{m}\delta_{fi}\boldsymbol{\epsilon}'_\gamma \cdot \boldsymbol{\epsilon}_\gamma + \sum_v \omega_{fv}\omega_{vi} \frac{\langle f|\boldsymbol{\epsilon}'_\gamma \cdot \mathbf{x}|v\rangle\langle v|\boldsymbol{\epsilon}_\gamma \cdot \mathbf{x}|i\rangle}{\omega_{vi} - ck - i\eta} \right. \\ &\left. + \sum_v \omega_{fv}\omega_{vi} \frac{\langle f|\boldsymbol{\epsilon}_\gamma \cdot \mathbf{x}|v\rangle\langle v|\boldsymbol{\epsilon}'_\gamma \cdot \mathbf{x}|i\rangle}{\omega_{vi} + ck' - i\eta} \right|_{\omega_{fi}=ck-ck'}^2. \end{aligned} \quad (76)$$

Textbook derivations of the scattering cross sections from the second order expansion of time-evolution operators can be found in [2, 5]. The structure of the denominators in the second and third terms in Eqs. (75,76) follows from the time integrals in the second order scattering matrix element,

$$\begin{aligned} &\int_{-\infty}^{\infty} dt \int_{-\infty}^t dt' \exp[i(\omega_{fv} + ck')t] \exp[i(\omega_{vi} - ck)t' + \eta t'] \\ &= -2\pi i \frac{\delta(\omega_{fi} + ck' - ck)}{\omega_{vi} - ck - i\eta}, \end{aligned} \quad (77)$$

$$\begin{aligned} &\int_{-\infty}^{\infty} dt \int_{-\infty}^t dt' \exp[i(\omega_{fv} - ck)t] \exp[i(\omega_{vi} + ck')t' + \eta t'] \\ &= -2\pi i \frac{\delta(\omega_{fi} + ck' - ck)}{\omega_{vi} + ck' - i\eta}. \end{aligned} \quad (78)$$

The shift $\omega_{vi} \rightarrow \omega_{vi} - i\eta$ can be understood as a consequence of $E_v \rightarrow E_v - i\hbar\eta$, i.e. η^{-1} is the decay time of the intermediate state $|v\rangle$.

The differential scattering cross section $d\sigma/d\Omega$ arises from differential transition rates into volume elements $d^3\mathbf{k}' = k'^2 dk' d\Omega$ of final photon states (normalized by incident photon flux), after integration over dk' against the energy conserving δ -function $\delta(\omega_{fi} + ck' - ck)$, see e.g. Eqs. (18.191-18.193) in [5]. However, it is also useful to consider the differential scattering cross section in

Wigner-Weisskopf form, $d\sigma/d\Omega dk'$, with substitution of a Lorentz profile $\Delta_\Gamma(\omega_{fi} + ck' - ck)$ (59) for the δ -function if lineshapes are resolved [16, 17],

$$\begin{aligned} \frac{d\sigma}{d\Omega dk'} &= \alpha_S^2 \frac{k'}{ck} \Delta_\Gamma(\omega_{fi} + ck' - ck) \left| \frac{\hbar}{m} \delta_{fi} \boldsymbol{\epsilon}'_\gamma \cdot \boldsymbol{\epsilon}_\gamma \right. \\ &+ \sum_v \omega_{fv} \omega_{vi} \frac{\langle f|\boldsymbol{\epsilon}'_\gamma \cdot \mathbf{x}|v\rangle\langle v|\boldsymbol{\epsilon}_\gamma \cdot \mathbf{x}|i\rangle}{\omega_{vi} - ck - i\eta} \\ &\left. + \sum_v \omega_{fv} \omega_{vi} \frac{\langle f|\boldsymbol{\epsilon}_\gamma \cdot \mathbf{x}|v\rangle\langle v|\boldsymbol{\epsilon}'_\gamma \cdot \mathbf{x}|i\rangle}{\omega_{vi} + ck' - i\eta} \right|^2. \end{aligned} \quad (79)$$

If the scattering is dominated by nearly resonant intermediate states, i.e. if we have states $|v\rangle$ such that

$$\langle f|\boldsymbol{\epsilon}'_\gamma \cdot \mathbf{x}|v\rangle\langle v|\boldsymbol{\epsilon}_\gamma \cdot \mathbf{x}|i\rangle \neq 0 \wedge \omega_{vi} - ck = \omega_{vf} - ck' \simeq 0 \quad (80)$$

or

$$\langle f|\boldsymbol{\epsilon}_\gamma \cdot \mathbf{x}|v\rangle\langle v|\boldsymbol{\epsilon}'_\gamma \cdot \mathbf{x}|i\rangle \neq 0 \wedge \omega_{vi} + ck' = \omega_{vf} + ck \simeq 0, \quad (81)$$

then $\omega_{fv}\omega_{vi} \simeq -c^2kk'$ and we can use the Kramers-Heisenberg approximations

$$\begin{aligned} \frac{d\sigma}{d\Omega} &= \alpha_S^2 c^2 k k'^3 \left| \sum_v \frac{\langle f|\boldsymbol{\epsilon}'_\gamma \cdot \mathbf{x}|v\rangle\langle v|\boldsymbol{\epsilon}_\gamma \cdot \mathbf{x}|i\rangle}{\omega_{vi} - ck - i\eta} \right. \\ &\left. + \sum_v \frac{\langle f|\boldsymbol{\epsilon}_\gamma \cdot \mathbf{x}|v\rangle\langle v|\boldsymbol{\epsilon}'_\gamma \cdot \mathbf{x}|i\rangle}{\omega_{vi} + ck' - i\eta} \right|_{\omega_{fi}=ck-ck'}^2 \end{aligned} \quad (82)$$

or

$$\begin{aligned} \frac{d\sigma}{d\Omega dk'} &= \alpha_S^2 c^3 k k'^3 \Delta_\Gamma(\omega_{fi} + ck' - ck) \\ &\times \left| \sum_v \frac{\langle f|\boldsymbol{\epsilon}'_\gamma \cdot \mathbf{x}|v\rangle\langle v|\boldsymbol{\epsilon}_\gamma \cdot \mathbf{x}|i\rangle}{\omega_{vi} - ck - i\eta} \right. \\ &\left. + \sum_v \frac{\langle f|\boldsymbol{\epsilon}_\gamma \cdot \mathbf{x}|v\rangle\langle v|\boldsymbol{\epsilon}'_\gamma \cdot \mathbf{x}|i\rangle}{\omega_{vi} + ck' - i\eta} \right|^2, \end{aligned} \quad (83)$$

respectively.

The Kramers-Heisenberg approximation follows directly from the Schrödinger equation if, instead of minimal coupling, we use a dipole coupling $H_{e\gamma} \simeq e\mathbf{x} \cdot \mathbf{E}(t)$ for the electron-photon interaction Hamiltonian, see e.g. [18, 19].

The abundance of energy states in many-electron systems and the inherent weakness of the $\mathcal{O}(\alpha_S^2)$ scattering signal imply that photon scattering in materials is always dominated by nearly resonant transitions through intermediate virtual states. This explains why the Kramers-Heisenberg approximation is ubiquitous in spectroscopy with synchrotron radiation [17, 20–26]. The Kramers-Heisenberg formula has been successfully applied e.g. to CaF₂ [27], lanthanum and lanthanum compounds [28–30] as well as compounds of other rare-earth elements [31–34], titanium and titanium compounds [35], cobalt compounds [36, 37], lithium fluoride [38], silicon and aluminum and their compounds [39–41], zinc oxide [42], aqueous solutions of transition metals [43, 44], and N₂ [45].

The second resonance condition (81) cannot be fulfilled if $|i\rangle$ is the ground state $|g\rangle$ of the scattering system, or if $E_i - E_g < \hbar ck'$. In these cases only the first term in Eq. (82) (which is known as the “resonant term”) is kept, while the second term (often denoted as the “non-resonant” or “anti-resonant” term) can be discarded.

We will display the corresponding scattering cross sections with continuous external electron states $|i\rangle$ or $|f\rangle$ only in the Kramers-Heisenberg approximation. The corresponding $\mathcal{O}(\alpha_S^2)$ correct formulae like (76) can be inferred from the corresponding Kramers-Heisenberg formulae through reversing the steps that led from (76) to (82).

B. Differential scattering cross section for $|i\rangle$ discrete and $|f\rangle$ continuous

This case applies e.g. to excitation of an electron from a donor level into the conduction band of a semiconductor if the energy absorption does not occur as a consequence of direct photon absorption (as described in Sec. III B), but through photon scattering. We formulate the corresponding Kramers-Heisenberg formula for the case that the final states reside in energy bands $E_n(\mathbf{k}_e)$, $|f\rangle = |n, \mathbf{k}_e\rangle$. A schematic involving resonantly enhanced scattering through intermediate energy band states is depicted in Fig. 8

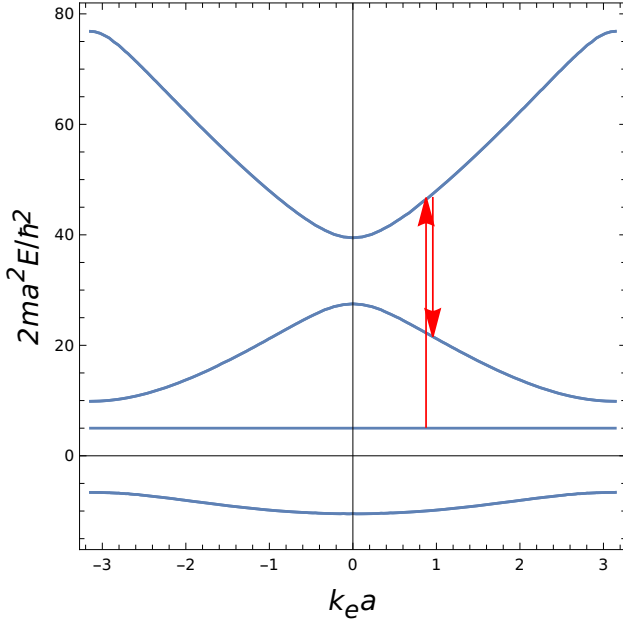


FIG. 8. Scattering from a \mathbf{k}_e -independent discrete atomic energy level into an energy band. In this case the scattering is resonantly enhanced through an intermediate band state. The depicted bands correspond to the lowest three energy bands in a Kronig-Penney model $V(x) = \mathcal{W} \sum_n \delta(x - na)$ with parameter $m\mathcal{W}a/\hbar^2 = -3$.

Transitions can involve intermediate and final Bloch

states with arbitrary wave vector \mathbf{k}_e , because the limit $\lambda_e \geq 2a$ on Bloch wavelengths implies that the plane wave factors vary slowly over the extent of the atomic wave functions. The emitting interband transition is a direct transition because the emitted photon wavelength satisfies $\lambda \gg 2a$ and therefore $k \ll \pi/a$, see Eq. (43).

The differential photon scattering cross section into $d\Omega dk'$ for the scattered photons implies an integration over the energy surface $E_f \equiv E_n(\mathbf{k}_e) = E_i + \hbar ck - \hbar ck'$ in the conduction band,

$$\begin{aligned} \frac{d\sigma}{d\Omega dk'} &= \alpha_S^2 \hbar c^3 k k'^3 \int_{E_n(\mathbf{k}_e)=E_i+\hbar ck-\hbar ck'} \frac{d^2 \mathbf{k}_{e\parallel}}{|\partial E_n(\mathbf{k}_e)/\partial \mathbf{k}_e|} \\ &\times \left| \sum_v \frac{\langle n, \mathbf{k}_e | \boldsymbol{\epsilon}'_\gamma \cdot \mathbf{x} | v \rangle \langle v | \boldsymbol{\epsilon}_\gamma \cdot \mathbf{x} | i \rangle}{\omega_{vi} - ck - i\eta} \right. \\ &\left. + \sum_v \frac{\langle n, \mathbf{k}_e | \boldsymbol{\epsilon}_\gamma \cdot \mathbf{x} | v \rangle \langle v | \boldsymbol{\epsilon}'_\gamma \cdot \mathbf{x} | i \rangle}{\omega_{vi} + ck' - i\eta} \right|^2. \end{aligned} \quad (84)$$

In this case, the assumption of approximately constant Kramers-Heisenberg dispersion factor across the constant energy surface relates the differential scattering cross section to the density of states (64),

$$\begin{aligned} \frac{d\sigma}{d\Omega dk'} &= \alpha_S^2 \hbar c^3 k k'^3 \rho_{n,V}(E_i + \hbar ck - \hbar ck') \\ &\times \left| \sum_v \frac{\langle u_n(\mathbf{k}_e) | \boldsymbol{\epsilon}'_\gamma \cdot \mathbf{x} | v \rangle \langle v | \boldsymbol{\epsilon}_\gamma \cdot \mathbf{x} | i \rangle}{\omega_{vi} - ck - i\eta} \right. \\ &\left. + \sum_v \frac{\langle u_n(\mathbf{k}_e) | \boldsymbol{\epsilon}_\gamma \cdot \mathbf{x} | v \rangle \langle v | \boldsymbol{\epsilon}'_\gamma \cdot \mathbf{x} | i \rangle}{\omega_{vi} + ck' - i\eta} \right|^2. \end{aligned} \quad (85)$$

Just as for the dipole factors in the absorption cross sections (62,63,69,70), the assumption of approximately constant dispersion factor across the constant energy surface $E_n(\mathbf{k}_e) = E_i + \hbar ck - \hbar ck'$ could be justified if that energy surface is small compared to the typical area dimension $4\pi^2/V^{2/3}$ of the Brillouin zone. The integral in (84) then spans a relatively small surface area in the Brillouin zone such that the intermediate and final Bloch wave functions do not vary a lot with \mathbf{k}_e .

For the contributions from intermediate Bloch states

$$|n', \mathbf{k}'_e\rangle = \sqrt{\frac{V}{8\pi^3}} \exp(i\mathbf{k}'_e \cdot \mathbf{x}) |u_{n'}(\mathbf{k}'_e)\rangle \quad (86)$$

to the sum over virtual intermediate states $|v\rangle$ in the dispersion factors, we note with (48) that

$$\begin{aligned} &\sum_{n'} \int d^3 \mathbf{k}'_e \langle n, \mathbf{k}_e | \boldsymbol{\epsilon}_\gamma \cdot \mathbf{p} | n', \mathbf{k}'_e \rangle \langle n', \mathbf{k}'_e | \dots \\ &= \sum_{n'} \langle u_n(\mathbf{k}_e) | \boldsymbol{\epsilon}_\gamma \cdot (\mathbf{p} + \hbar \mathbf{k}_e) | u_{n'}(\mathbf{k}_e) \rangle_V \langle n', \mathbf{k}_e | \dots \\ &= i \frac{m}{\hbar} \sum_{n'} \langle u_n(\mathbf{k}_e) | \boldsymbol{\epsilon}_\gamma \cdot [H_0(\mathbf{k}_e), \mathbf{x}] | u_{n'}(\mathbf{k}_e) \rangle_V \\ &\quad \times \langle n', \mathbf{k}_e | \dots, \end{aligned} \quad (87)$$

where

$$H_0(\mathbf{k}_e) = \frac{1}{2m}(\mathbf{p} + \hbar\mathbf{k}_e)^2 + V(\mathbf{x}) \quad (88)$$

is the lattice Hamiltonian for the periodic Bloch factors $\langle \mathbf{x} | u_n(\mathbf{k}_e) \rangle$. This implies that the contribution from the intermediate virtual band states to the scattering cross section amounts to a summation over band states with the same electron wave vector \mathbf{k}_e . Furthermore, the matrix element of the Bloch states reduces to an integral over the Wigner-Seitz cell, where the Bloch wave functions $\langle \mathbf{x} | n, \mathbf{k}_e \rangle$ are replaced with the corresponding Bloch factors $\langle \mathbf{x} | u_n(\mathbf{k}_e) \rangle$.

C. Differential scattering cross section for $|i\rangle$ continuous and $|f\rangle$ discrete

This case would apply e.g. to a case where an electron is promoted from a valence band state into an acceptor state through photon scattering instead of straight photon absorption. We therefore use valence band states as initial states, $|i\rangle = |n, \mathbf{k}_e\rangle$. A schematic involving resonantly enhanced scattering through intermediate energy band states is depicted in Fig. 9

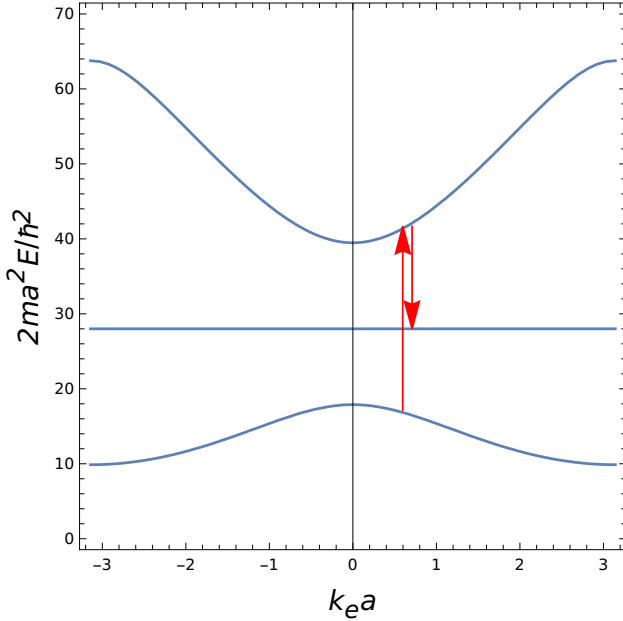


FIG. 9. Scattering into a \mathbf{k}_e -independent discrete atomic energy level. In this case the scattering is resonantly enhanced through an intermediate band state. The depicted bands correspond to the second and third energy band in a Kronig-Penney model $V(x) = \mathcal{W} \sum_n \delta(x - na)$ with parameter $m\mathcal{W}a/\hbar^2 = -7$.

Transitions can involve initial and intermediate Bloch states with arbitrary wave vector \mathbf{k}_e , because the limit $\lambda_e \geq 2a$ on Bloch wavelengths implies that the plane wave factors vary slowly over the extent of the atomic

wave functions. The absorbing interband transition is a direct transition because the emitted photon wavelength satisfies $\lambda \gg 2a$ and therefore $k \ll \pi/a$, see Eq. (43).

The differential photon scattering cross section into $d\Omega dk'$ for the scattered photons implies an integration over the energy surface $E_i \equiv E_n(\mathbf{k}_e) = E_f + \hbar ck' - \hbar ck$ in the valence band,

$$\begin{aligned} \frac{d\sigma}{d\Omega dk'} &= \alpha_S^2 \hbar c^3 k k'^3 \int_{E_n(\mathbf{k}_e)=E_f+\hbar ck'-\hbar ck} \frac{d^2 \mathbf{k}_{e\parallel}}{|\partial E_n(\mathbf{k}_e)/\partial \mathbf{k}_e|} \\ &\times \left| \sum_v \frac{\langle f | \boldsymbol{\epsilon}'_\gamma \cdot \mathbf{x} | v \rangle \langle v | \boldsymbol{\epsilon}_\gamma \cdot \mathbf{x} | n, \mathbf{k}_e \rangle}{\omega_{vi} - ck - i\eta} \right. \\ &\left. + \sum_v \frac{\langle f | \boldsymbol{\epsilon}_\gamma \cdot \mathbf{x} | v \rangle \langle v | \boldsymbol{\epsilon}'_\gamma \cdot \mathbf{x} | n, \mathbf{k}_e \rangle}{\omega_{vi} + ck' - i\eta} \right|^2, \quad (89) \end{aligned}$$

and the assumption of approximately constant dispersion factor relates this again to the density of states (64),

$$\begin{aligned} \frac{d\sigma}{d\Omega dk'} &= \alpha_S^2 \hbar c^3 k k'^3 \rho_{n,V}(E_f + \hbar ck' - \hbar ck) \\ &\times \left| \sum_v \frac{\langle f | \boldsymbol{\epsilon}'_\gamma \cdot \mathbf{x} | v \rangle \langle v | \boldsymbol{\epsilon}_\gamma \cdot \mathbf{x} | u_n(\mathbf{k}_e) \rangle}{\omega_{vi} - ck - i\eta} \right. \\ &\left. + \sum_v \frac{\langle f | \boldsymbol{\epsilon}_\gamma \cdot \mathbf{x} | v \rangle \langle v | \boldsymbol{\epsilon}'_\gamma \cdot \mathbf{x} | u_n(\mathbf{k}_e) \rangle}{\omega_{vi} + ck' - i\eta} \right|^2. \quad (90) \end{aligned}$$

The observations (87,88) concerning the contributions from intermediate virtual band states also apply here.

D. Differential scattering cross section for both $|i\rangle$ and $|f\rangle$ continuous

This applies e.g. to photon scattering off free electrons. The resonance conditions (80) or (81) cannot be fulfilled in this case and the elastic Thomson scattering term (the first term in Eq. (75)) dominates low-energy photon scattering off free electrons. The factor δ_{fi} in the discrete-to-discrete Thomson term in (75) is replaced with $\int d^3 \mathbf{k}'_e \delta(\mathbf{k}'_e - \mathbf{k}_e) \delta(\mathbf{0}) 8\pi^3/\mathcal{V} = 1$ for scattering of free electrons with initial momentum $\hbar \mathbf{k}_e$ into outgoing momentum eigenstates $|f\rangle = |\mathbf{k}'_e\rangle$. This yields the well-known result

$$\frac{d\sigma}{d\Omega} = \left(\frac{\alpha_S \hbar}{mc} \right)^2 (\boldsymbol{\epsilon}'_\gamma \cdot \boldsymbol{\epsilon}_\gamma)^2. \quad (91)$$

The Kramers-Heisenberg dispersion terms provide corrections to the Thomson term which in leading order scale like $\mathcal{O}(\hbar k/mc)$. However, the quantum optics result (75) is not useful for calculating corrections to Thomson scattering off free electrons because Compton scattering is dealt with by the Klein-Nishina formula.

On the other hand, scattering between continuous initial and final electron states also applies to scattering between energy bands $|i\rangle = |n, \mathbf{k}_e\rangle \rightarrow |f\rangle = |n', \mathbf{k}_e\rangle$, where dipole approximation yields again direct interband

transitions $\mathbf{k}'_e = \mathbf{k}_e$. Adapting the Kramers-Heisenberg relation to this situation became important with the availability of synchrotron light sources for inelastic X-ray scattering between energy bands in materials [20–23]. A schematic involving resonantly enhanced scattering through intermediate energy band states is depicted in Fig. 10

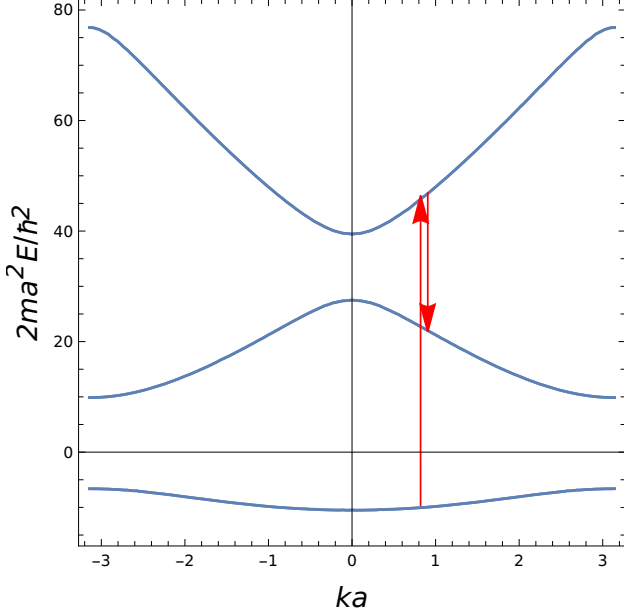


FIG. 10. Scattering between energy bands. In this case the scattering is resonantly enhanced through an intermediate band state. The depicted bands correspond to the lowest three energy bands in a Kronig-Penney model $V(x) = \mathcal{W} \sum_n \delta(x - na)$ with parameter $m\mathcal{W}a/\hbar^2 = -3$. The interband transitions are direct transitions because the photon wave vectors satisfy $k \ll \pi/a$.

The scattering cross section in the Kramers-Heisenberg approximation with scattering through intermediate band states $|v, \mathbf{k}'_e\rangle$ is

$$\begin{aligned} \frac{d\sigma}{d\Omega} &= \alpha_S^2 c^2 k k'^3 \quad (92) \\ &\times \left| \sum_v \frac{\langle u_{n'}(\mathbf{k}_e) | \boldsymbol{\epsilon}'_\gamma \cdot \mathbf{x} | u_v(\mathbf{k}_e) \rangle_V \langle u_v(\mathbf{k}_e) | \boldsymbol{\epsilon}_\gamma \cdot \mathbf{x} | u_n(\mathbf{k}_e) \rangle_V}{\omega_{v,n}(\mathbf{k}_e) - ck - i\eta} \right. \\ &\left. + \sum_v \frac{\langle u_{n'}(\mathbf{k}_e) | \boldsymbol{\epsilon}_\gamma \cdot \mathbf{x} | u_v(\mathbf{k}_e) \rangle_V \langle u_v(\mathbf{k}_e) | \boldsymbol{\epsilon}'_\gamma \cdot \mathbf{x} | u_n(\mathbf{k}_e) \rangle_V}{\omega_{v,n}(\mathbf{k}_e) + ck' - i\eta} \right|^2, \end{aligned}$$

where $ck' = ck - \omega_{n',n}(\mathbf{k}_e)$ and Eqs. (48,87) imply that all transitions occur at the same point \mathbf{k}_e in the Brillouin zone.

The differential scattering cross section per lattice cell for transitions from a valence band $E_n(\mathbf{k}_e)$ into a con-

duction band $E_{n'}(\mathbf{k}_e)$ is

$$\begin{aligned} \frac{d\sigma}{d\Omega dk'} &= \alpha_S^2 \hbar c^3 k k'^3 \frac{V}{8\pi^3} \quad (93) \\ &\times \int_{E_{n'}(\mathbf{k}_e) - E_n(\mathbf{k}_e) = \hbar c(k - k')} \frac{d^2 \mathbf{k}_{e\parallel}}{|\partial[E_{n'}(\mathbf{k}_e) - E_n(\mathbf{k}_e)]/\partial \mathbf{k}_e|} \\ &\times \left| \sum_v \frac{\langle u_{n'}(\mathbf{k}_e) | \boldsymbol{\epsilon}'_\gamma \cdot \mathbf{x} | u_v(\mathbf{k}_e) \rangle_V \langle u_v(\mathbf{k}_e) | \boldsymbol{\epsilon}_\gamma \cdot \mathbf{x} | u_n(\mathbf{k}_e) \rangle_V}{\omega_{v,n}(\mathbf{k}_e) - ck - i\eta} \right. \\ &\left. + \sum_v \frac{\langle u_{n'}(\mathbf{k}_e) | \boldsymbol{\epsilon}_\gamma \cdot \mathbf{x} | u_v(\mathbf{k}_e) \rangle_V \langle u_v(\mathbf{k}_e) | \boldsymbol{\epsilon}'_\gamma \cdot \mathbf{x} | u_n(\mathbf{k}_e) \rangle_V}{\omega_{v,n}(\mathbf{k}_e) + ck' - i\eta} \right|^2. \end{aligned}$$

We can express this through the joint density of states (74) at the energy transfer $\Delta E = \hbar c(k - k')$ if the Kramers-Heisenberg dispersion factor is approximately constant over the constant energy surface $E_{n'}(\mathbf{k}_e) - E_n(\mathbf{k}_e) = \hbar c(k - k')$,

$$\begin{aligned} \frac{d\sigma}{d\Omega dk'} &= \alpha_S^2 \hbar c^3 k k'^3 \varrho_{n',n,V}(\hbar ck - \hbar ck') \quad (94) \\ &\times \left| \sum_v \frac{\langle u_{n'}(\mathbf{k}_e) | \boldsymbol{\epsilon}'_\gamma \cdot \mathbf{x} | u_v(\mathbf{k}_e) \rangle_V \langle u_v(\mathbf{k}_e) | \boldsymbol{\epsilon}_\gamma \cdot \mathbf{x} | u_n(\mathbf{k}_e) \rangle_V}{\omega_{v,n}(\mathbf{k}_e) - ck - i\eta} \right. \\ &\left. + \sum_v \frac{\langle u_{n'}(\mathbf{k}_e) | \boldsymbol{\epsilon}_\gamma \cdot \mathbf{x} | u_v(\mathbf{k}_e) \rangle_V \langle u_v(\mathbf{k}_e) | \boldsymbol{\epsilon}'_\gamma \cdot \mathbf{x} | u_n(\mathbf{k}_e) \rangle_V}{\omega_{v,n}(\mathbf{k}_e) + ck' - i\eta} \right|^2. \end{aligned}$$

V. CONCLUSIONS

The leading order equations for photon emission have been summarized in Sec. II, for photon absorption in Sec. III, and for photon scattering in Sec. IV. In each section, the different cases of discrete-to-discrete, discrete-to-continuous, continuous-to-discrete and continuous-to-continuous electronic transitions have been described in separate subsections. The different cases of photon transitions differ in terms of the quantity that is calculated as a measure for the transition: emission rates for photon emission, absorption cross sections for photon absorption, and scattering cross sections for photon scattering. The different cases of electronic transitions differ in the appropriate factors for incoming and outgoing electronic states in terms of densities of states or joint densities of states, or through integrations over \mathbf{k}_e -space, if continuous states are involved. This compendium can hopefully serve as a concise manual for the many researchers who navigate the landscape of radiative transition equations for their work in spectroscopy, quantum optics, or photonics.

Appendix A: Continuous states

Ionization of materials and ion-electron recombination involve states in the continuous energy spectrum of a material. Transitions in materials which involve energy

bands also involve states in an energy continuum. Equations for transitions involving continuous states, e.g. the Golden Rule, are often expressed in terms of densities of states in the energy scale. However, transition probabilities between energy bands in condensed materials are more commonly derived in terms of the quasiperiodic Bloch energy eigenstates $|n, \mathbf{k}_e\rangle$,

$$\begin{aligned} \langle \mathbf{x} | n, \mathbf{k}_e \rangle &= \psi_n(\mathbf{k}_e, \mathbf{x}) \\ &= \sqrt{\frac{V}{8\pi^3}} \exp(i\mathbf{k}_e \cdot \mathbf{x}) u_n(\mathbf{k}_e, \mathbf{x}), \end{aligned} \quad (\text{A1})$$

where V is the volume of the Wigner-Seitz cell and $u_n(\mathbf{k}_e, \mathbf{x})$ are the periodic Bloch factors for the energy band $E_n(\mathbf{k}_e)$. The Bloch energy eigenfunctions $\psi_n(\mathbf{k}_e, \mathbf{x})$ are periodically perturbed plane waves with normalization

$$\langle n', \mathbf{k}'_e | n, \mathbf{k}_e \rangle = \delta_{nn'} \delta(\mathbf{k}_e - \mathbf{k}'_e). \quad (\text{A2})$$

We extract the factor $\sqrt{V/8\pi^3}$ from the Bloch factors, because with this definition the property (A2) of the Bloch energy eigenfunctions implies normalization of the periodic Bloch factors $\langle \mathbf{x} | u_n(\mathbf{k}_e) \rangle = u_n(\mathbf{k}_e, \mathbf{x})$ to the Wigner-Seitz cell,

$$\begin{aligned} \langle n', \mathbf{k}'_e | n, \mathbf{k}_e \rangle_V &\equiv \int_V d^3\mathbf{x} u_{n'}^+(\mathbf{k}'_e, \mathbf{x}) u_n(\mathbf{k}_e, \mathbf{x}) \\ &= \delta_{nn'}, \end{aligned} \quad (\text{A3})$$

where the integration is over the Wigner-Seitz cell and both Bloch factors must refer to the same wave vector \mathbf{k}_e in the Brillouin zone.

The connections between densities of states in the energy scale and wave vector parametrizations for continuous states are encoded in the completeness relations, which involve sums over the discrete energy eigenvalues E_j and the continuous parts C of the spectrum,

$$\begin{aligned} 1 &= \sum_{j,\nu} |E_j, \nu\rangle \langle E_j, \nu| \\ &+ \sum_{\nu} \int_C dE |E, \nu\rangle \tilde{\varrho}(E, \nu) \langle E, \nu| \end{aligned} \quad (\text{A4})$$

$$\begin{aligned} &= \sum_{j,\nu} |E_j, \nu\rangle \langle E_j, \nu| \\ &+ \sum_n \int_{\mathcal{B}} d^3\mathbf{k}_e |n, \mathbf{k}_e\rangle \langle n, \mathbf{k}_e|. \end{aligned} \quad (\text{A5})$$

The integral $\int_{\mathcal{B}} d^3\mathbf{k}_e \dots$ covers the first Brillouin zone. The energy integral $\int_C dE \dots$ covers all the continuous energy eigenvalues, i.e. in a condensed material the integration domain $C = \sum_n \oplus C_n$ covers all the energy bands. The sum \sum_{ν} over degeneracy indices for the energy eigenstates $|E, \nu\rangle$ in the continuous part C of the spectrum can involve summations over discrete quantum numbers or integrations over continuous quantum numbers.

The contribution from the energy band $E_n(\mathbf{k}_e)$ to the density of states follows from

$$d^3\mathbf{k}_e = d^2\mathbf{k}_{e\parallel} dk_{e,\perp} \rightarrow d^2\mathbf{k}_{e\parallel} \frac{dE}{|\partial E_n(\mathbf{k}_e)/\partial \mathbf{k}_e|}, \quad (\text{A6})$$

where $d^2\mathbf{k}_{e\parallel}$ denotes an integration measure on the surface of constant energy $E_n(\mathbf{k}_e)$. This implies

$$\begin{aligned} &\int_{\mathcal{B}} d^3\mathbf{k}_e |n, \mathbf{k}_e\rangle \langle n, \mathbf{k}_e| \\ &\rightarrow \int_{C_n} dE \int_{E_n(\mathbf{k}_e)=E} d^2\mathbf{k}_{e\parallel} \frac{|n, \mathbf{k}_e\rangle \langle n, \mathbf{k}_e|}{|\partial E_n(\mathbf{k}_e)/\partial \mathbf{k}_e|}. \end{aligned} \quad (\text{A7})$$

If we agree to use the continuous variables included in the integration measure $d^2\mathbf{k}_{e\parallel}$ as degeneracy indices ν , $\sum_{\nu} \rightarrow \int d^2\mathbf{k}_{e\parallel}$, and set $|E, \mathbf{k}_{\parallel}\rangle = |n, \mathbf{k}_e\rangle$ for $E = E_n(\mathbf{k}_e)$, comparison of (A7) with (A4) tells us that the contribution from the energy band $E_n(\mathbf{k})$ to the partial density of states $\tilde{\varrho}(E, \nu) = \sum_n \tilde{\varrho}_n(E, \nu)$ is

$$\tilde{\varrho}_n(E, \nu) \equiv \tilde{\varrho}_n(E, \mathbf{k}_{\parallel}) = \frac{1}{|\partial E_n(\mathbf{k}_e)/\partial \mathbf{k}_e|}. \quad (\text{A8})$$

The normalization of $\tilde{\varrho}(E, \nu)$ depends on the normalization of the continuous states $|E, \nu\rangle$. The expression (14) for energies in the continuous part of the spectrum,

$$\varrho(E, \mathbf{x}) dE = \sum_{\nu} \langle \mathbf{x} | E, \nu \rangle \tilde{\varrho}(E, \nu) \langle E, \nu | \mathbf{x} \rangle dE \quad (\text{A9})$$

gives the local density of continuous states per volume V at location \mathbf{x} and with energies in the interval $[E, E+dE]$, i.e. scaling the states $|E, \nu\rangle$ with a factor ξ scales $\tilde{\varrho}(E, \nu)$ by $|\xi|^{-2}$.

We can switch from the *a priori* continuous degeneracy indices ν_c , which provide coordinates on the constant energy surface, to discrete indices ν_d through harmonic analysis,

$$\int d^2\nu_c |E, \nu_c\rangle \tilde{\varrho}(E, \nu_c) \langle E, \nu_c| = \sum_{\nu_d} |E, \nu_d\rangle \tilde{\varrho}(E, \nu_d) \langle E, \nu_d|.$$

Both parametrizations will yield the same local density of states $\varrho(E, \mathbf{x})$. The local density of states (per spin state) for nonrelativistic free electrons with plane wave states $|\mathbf{k}_e\rangle$ is

$$\begin{aligned} \varrho_e(E, \mathbf{x}) &= \int_{E(\mathbf{k}_e)=E} d^2\mathbf{k}_{e\parallel} \frac{|\langle \mathbf{x} | \mathbf{k}_e \rangle|^2}{|\partial E(\mathbf{k}_e)/\partial \mathbf{k}_e|} \\ &= \frac{1}{8\pi^3} \int_{E(\mathbf{k}_e)=E} \frac{d^2\mathbf{k}_{e\parallel}}{|\partial E(\mathbf{k}_e)/\partial \mathbf{k}_e|} \\ &= \frac{\Theta(E)}{2\pi^2 \hbar^3} \sqrt{2m^3 E}, \end{aligned} \quad (\text{A10})$$

and this is independent of position. However, the local density of electron states (per spin state) in the energy band $E_n(\mathbf{k}_e)$ involves the Bloch factors,

$$\varrho_n(E, \mathbf{x}) = \frac{V}{8\pi^3} \int_{E_n(\mathbf{k}_e)=E} d^2\mathbf{k}_{e\parallel} \frac{|u_n(\mathbf{k}_e, \mathbf{x})|^2}{|\partial E(\mathbf{k}_e)/\partial \mathbf{k}_e|}, \quad (\text{A11})$$

where V is the volume of the Wigner-Seitz cell. The density of states (64) emerges from the local density of states (A11) after integration over a Wigner-Seitz cell,

$$\varrho_{n,V}(E) = \int_V d^3\mathbf{x} \varrho_n(E, \mathbf{x}). \quad (\text{A12})$$

Appendix B: The quantum fields in the quantum optics Hamiltonian

The electron field $\Psi_s(\mathbf{x}, t)$ and the photon field $\mathbf{A}(\mathbf{x}, t)$ in the Coulomb gauge Hamiltonian (1-6) are quantum fields in the Heisenberg picture which are related to the time-independent quantum fields of the Schrödinger picture through

$$\Psi_s(\mathbf{x}, t) = \exp(iHt/\hbar)\Psi_s(\mathbf{x})\exp(-iHt/\hbar), \quad (\text{B1})$$

$$\mathbf{A}(\mathbf{x}, t) = \exp(iHt/\hbar)\mathbf{A}(\mathbf{x})\exp(-iHt/\hbar). \quad (\text{B2})$$

Canonical quantization implies the anticommutation relations for electron operators

$$\{\Psi_s(\mathbf{x}), \Psi_{s'}^\dagger(\mathbf{x}')\} = \delta(\mathbf{x} - \mathbf{x}'), \quad \{\Psi_s(\mathbf{x}), \Psi_{s'}(\mathbf{x}')\} = 0,$$

and commutation relations for photon operators (with $E_i(\mathbf{x}) = -\dot{A}_i(\mathbf{x}, t)|_{t \rightarrow 0}$)

$$[A_i(\mathbf{x}), E_j(\mathbf{x}')] = -\frac{i\hbar}{\epsilon_0}\delta_{ij}^\perp(\mathbf{x} - \mathbf{x}'), \quad (\text{B3})$$

$$[A_i(\mathbf{x}), A_j(\mathbf{x}')] = 0, \quad [E_i(\mathbf{x}), E_j(\mathbf{x}')] = 0, \quad (\text{B4})$$

where

$$\delta_{ij}^\perp(\mathbf{x}) = \frac{1}{(2\pi)^3} \int d^3\mathbf{k} \left(\delta_{ij} - \frac{k_i k_j}{k^2} \right) \exp(i\mathbf{k} \cdot \mathbf{x}) \quad (\text{B5})$$

is the transverse δ function.

The mode expansion of $A_i(\mathbf{x})$ contains the photon operators $a_\alpha^\pm(\mathbf{k})$ which create photons with momentum $\hbar\mathbf{k}$ and polarization $\epsilon_\alpha(\mathbf{k})$,

$$\begin{aligned} \mathbf{A}(\mathbf{x}) = & \sqrt{\frac{\hbar\mu_0 c}{8\pi^3}} \int \frac{d^3\mathbf{k}}{\sqrt{2k}} \sum_{\alpha=1}^2 \epsilon_\alpha(\mathbf{k}) \left(a_\alpha(\mathbf{k}) \exp(i\mathbf{k} \cdot \mathbf{x}) \right. \\ & \left. + a_\alpha^\dagger(\mathbf{k}) \exp(-i\mathbf{k} \cdot \mathbf{x}) \right). \end{aligned} \quad (\text{B6})$$

The electron creation operators $\Psi_s^\dagger(\mathbf{x})$ create e.g. single-electron states with spinor components $\psi_s(\mathbf{x}, t)$ through

$$|\psi(t)\rangle = \sum_s \int d^3\mathbf{x} \Psi_s^\dagger(\mathbf{x}) |0\rangle \psi_s(\mathbf{x}, t), \quad (\text{B7})$$

or general many-electron states,

$$\begin{aligned} |\psi(t)\rangle = & \sum_{s, s', \dots} \int d^3\mathbf{x} \int d^3\mathbf{x}' \Psi_s^\dagger(\mathbf{x}) \Psi_{s'}^\dagger(\mathbf{x}') \dots |0\rangle \\ & \times \psi_{s, s', \dots}(\mathbf{x}, \mathbf{x}', \dots, t). \end{aligned} \quad (\text{B8})$$

The many-electron states (B8) are usually approximated through products of orthonormalized single-electron states,

$$\begin{aligned} \psi_{s_1, s_2, \dots, s_N}(\mathbf{x}_1, \mathbf{x}_2, \dots, \mathbf{x}_N, t) \rightarrow & \psi_{n_1, s_1}(\mathbf{x}_1, t) \\ \times \psi_{n_2, s_2}(\mathbf{x}_2, t) \dots \psi_{n_N, s_N}(\mathbf{x}_N, t). \end{aligned} \quad (\text{B9})$$

The many-particle state in a material can then be thought of as the product of a many-electron state of the form (B8, B9) with corresponding many-particle states for the pertinent nuclei. The expectation value of the kinetic electron energy operator \mathcal{H}_e (2) for the many-particle state of the material then generates the sum of the kinetic energy densities of all the fundamental nonrelativistic electrons, and the expectation value of the potential operator for the electrons, i.e. the sum of relevant terms from (5),

$$\begin{aligned} \mathcal{V}_e(\mathbf{x}) = & \int d^3\mathbf{x}' \mathcal{H}_{ee}(\mathbf{x}, \mathbf{x}') \\ & + 2 \sum_{b=\text{nuclei}} \int d^3\mathbf{x}' \mathcal{H}_{eb}(\mathbf{x}, \mathbf{x}'), \end{aligned} \quad (\text{B10})$$

generates an effective single-electron potential. We use the Schrödinger picture in (B10), such that the wave functions in our many-particle quantum states are time-dependent but the operators are time-independent, see (B8).

The Coulomb terms in (5) automatically generate the exchange interaction terms in $\langle \mathcal{V}_e(\mathbf{x}) \rangle$ through Fermi statistics, but for realistic potentials in materials we would also have to include first order relativistic corrections like spin-orbit coupling. Furthermore, instead of summation over bare nuclei, we may decide to allocate core electrons to the nuclei and not count them separately towards the electronic states in the material, in the interest of efficiency. However, these details do not impact the spectroscopic formulae in this paper. The important observation is that even in a complex material we are still considering fundamental electrons which are moving in a potential, e.g. a periodic lattice potential in a solid material, and that couple to photons through the minimal coupling terms $\mathcal{H}_{e\gamma}$ (6) where $m = m_e$ is the electron mass. Furthermore, these electrons are described on the quantum mechanical level by the Hamiltonian (8) with an effective potential $V(\mathbf{x})$, such that (7) still holds. Eq. (8) and the transition between velocity and length form would not hold anymore if we have to take into account relativistic corrections to the kinetic energy, e.g. for deep core electrons in materials with heavy atoms.

The representation of the \mathbf{x} -space electron operators in terms of free \mathbf{k}_e -space electron operators is

$$\Psi_s(\mathbf{x}) = \frac{1}{\sqrt{2\pi^3}} \int d^3\mathbf{k}_e \exp(i\mathbf{k}_e \cdot \mathbf{x}) a_s(\mathbf{k}_e). \quad (\text{B11})$$

The corresponding representation for electrons in peri-

odic potentials is

$$\Psi_s(\mathbf{x}) = \sqrt{\frac{V}{8\pi^3}} \sum_n \int_{\mathcal{B}} d^3\mathbf{k}_e \exp(i\mathbf{k}_e \cdot \mathbf{x}) \times u_n(\mathbf{k}_e, \mathbf{x}) a_{n,s}(\mathbf{k}_e), \quad (\text{B12})$$

where n labels the energy bands, V is the volume of the Wigner-Seitz cell, $u_n(\mathbf{k}_e, \mathbf{x})$ is the Bloch factor with normalization (46), and the integration is over the Brillouin zone \mathcal{B} .

However, in both cases we are still dealing with electrons which couple to photons through the quantum optics interaction (6). The inversion of (B12),

$$a_{n,s}(\mathbf{k}_e) = \sqrt{\frac{V}{8\pi^3}} \int d^3\mathbf{x} \exp(-i\mathbf{k}_e \cdot \mathbf{x}) \times u_n^+(\mathbf{k}_e, \mathbf{x}) \Psi_s(\mathbf{x}), \quad (\text{B13})$$

provides the unitary transformation from the free electron operators in \mathbf{k}_e -space to the operators $a_{n,s}(\mathbf{k}_e)$ for electrons in energy bands,

$$a_{n,s}(\mathbf{k}_e) = \frac{\sqrt{V}}{8\pi^3} \int d^3\mathbf{x} \int d^3\mathbf{k}'_e \exp[i(\mathbf{k}'_e - \mathbf{k}_e) \cdot \mathbf{x}] \times u_n^+(\mathbf{k}_e, \mathbf{x}) a_s(\mathbf{k}'_e). \quad (\text{B14})$$

The different \mathbf{k}_e -space operators correspond to different convenient representations of electron operators depending on whether the electrons are moving freely or in a periodic potential.

With respect to the momenta of electrons moving in a periodic potential, we note that the equation for free electrons, $\langle \mathbf{k}'_e | \mathbf{p} | \mathbf{k}_e \rangle = \hbar \mathbf{k}_e \delta(\mathbf{k}_e - \mathbf{k}'_e)$ gets modified to

$$\langle n, \mathbf{k}'_e | \mathbf{p} | n, \mathbf{k}_e \rangle = \delta(\mathbf{k}_e - \mathbf{k}'_e) \times \left(\hbar \mathbf{k}_e + \int_V d^3\mathbf{x} u_n^+(\mathbf{k}_e, \mathbf{x}) \frac{\hbar}{i} \frac{\partial}{\partial \mathbf{x}} u_n(\mathbf{k}_e, \mathbf{x}) \right), \quad (\text{B15})$$

where the remaining integration on the right hand side is over the Wigner-Seitz cell. The limitation of translation symmetry to lattice vectors due to the periodic lattice potential implies that the energy eigenstates are not momentum eigenstates anymore. However, \mathbf{p} is still the first-quantized momentum operator for the electrons in the Bloch energy eigenstates.

We gave the Schrödinger picture electron states with their time-dependence in Eqs. (B7,B8). However, the states only enter for time $t = 0$ into the transition matrix elements, because the unperturbed time evolution operators $U_0(t, 0)$ from the external states transform the full time evolution operator in the scattering matrix elements into the time evolution operator of the interaction picture, evaluated between states at time $t = 0$.

Note that the bold-face kets in (B7,B8) correspond to Fock space states, which appear in the derivations of the transition amplitudes reported in the body of this review, but not in the final results. The kets in the transition amplitudes in Secs. II-IV correspond to the wave functions of the first quantized theory that enter into the matrix elements, e.g. $\psi_s(\mathbf{x}) = \langle \mathbf{x} | \psi_s \rangle$.

Appendix C: Atomic recoil

Recoils are usually neglected in transition matrix elements involving discrete atomic states. Recoil effects will be more prominent for transitions involving free atoms than for atoms which are bound into a molecule or a lattice. We will therefore discuss recoils between states of free atoms.

In a description of single electrons moving in an effective potential $V(\mathbf{x}_e - \mathbf{x}_p)$ created by the nucleus at position \mathbf{x}_p (the notation is motivated by exactness of these considerations for hydrogen atoms) and a radially symmetric distribution of the other electrons, the eigenstates can be written in the form

$$\langle \mathbf{x}_e, \mathbf{x}_p | \mathbf{K}, n \rangle = \frac{1}{\sqrt{2\pi^3}} \exp\left(i\mathbf{K} \cdot \frac{m_p \mathbf{x}_p + m_e \mathbf{x}_e}{m_p + m_e}\right) \times \psi_n(\mathbf{x}_e - \mathbf{x}_p). \quad (\text{C1})$$

Here $\hbar \mathbf{K}$ is the center-of-mass momentum and n represents the remaining set of orbital and spin quantum numbers of this effective two-particle problem. The mass $m_p \gg m_e$ includes the mass of the nucleus. The energy of the state (C1) is

$$E_n(\mathbf{K}) = \frac{\hbar^2 \mathbf{K}^2}{2(m_p + m_e)} + \hbar \omega_n. \quad (\text{C2})$$

Scattering matrix elements for transitions $|\mathbf{K}_i, n_i\rangle \rightarrow |\mathbf{K}_f, n_f\rangle$ due to electron-photon coupling then involve transition matrix elements

$$\begin{aligned} & \langle \mathbf{K}_f, n_f | \exp(-i\mathbf{k} \cdot \mathbf{x}_e) \epsilon_\gamma^+(\mathbf{k}) \cdot \frac{\mathbf{p}_e}{m_e} | \mathbf{K}_i, n_i \rangle \\ &= \int \frac{d^3\mathbf{x}_p}{(2\pi)^3} \int d^3\mathbf{x}_e \exp\left(i(\mathbf{K}_i - \mathbf{K}_f) \cdot \frac{m_p \mathbf{x}_p + m_e \mathbf{x}_e}{m_p + m_e}\right) \\ & \times \psi_f^+(\mathbf{x}_e - \mathbf{x}_p) \exp(-i\mathbf{k} \cdot \mathbf{x}_e) \\ & \times \epsilon_\gamma^+(\mathbf{k}) \cdot \left(\frac{\hbar}{im_e} \frac{\partial}{\partial \mathbf{x}_e} + \frac{m_e \hbar \mathbf{K}_i}{m_p + m_e} \right) \psi_i(\mathbf{x}_e - \mathbf{x}_p). \quad (\text{C3}) \end{aligned}$$

With regard to the photon terms, this is formulated for the case of emission of a real or virtual photon through this matrix element, but the argument of negligibility of atomic recoils given below is equally valid for the substitutions which correspond to photon absorption, $\epsilon_\gamma^+(\mathbf{k}) \rightarrow \epsilon_\gamma(\mathbf{k})$, $\exp(-i\mathbf{k} \cdot \mathbf{x}_e) \rightarrow \exp(i\mathbf{k} \cdot \mathbf{x}_e)$.

In the next step, we substitute center of mass and relative coordinates

$$\mathbf{X} = \frac{m_p \mathbf{x}_p + m_e \mathbf{x}_e}{m_p + m_e}, \quad \mathbf{x} = \mathbf{x}_e - \mathbf{x}_p, \quad (\text{C4})$$

$$\mathbf{x}_e = \mathbf{X} + \frac{m_p}{m_p + m_e} \mathbf{x}, \quad (\text{C5})$$

$$\frac{\partial}{\partial \mathbf{x}_e} = \frac{\partial}{\partial \mathbf{x}} + \frac{m_e}{m_p + m_e} \frac{\partial}{\partial \mathbf{X}}, \quad (\text{C6})$$

use dipole approximation in the atomic state matrix element,

$$\exp\left(-i\mathbf{k} \cdot \frac{m_p}{m_p + m_e} \mathbf{x}\right) \rightarrow 1, \quad (\text{C7})$$

and use orthogonality of the initial and final states, $\langle \mathbf{K}_f, n_f | \mathbf{K}_i, n_i \rangle = 0$, to find in dipole approximation

$$\begin{aligned} & \langle \mathbf{K}_f, n_f | \exp(-i\mathbf{k} \cdot \mathbf{x}_e) \boldsymbol{\epsilon}_\gamma^+(\mathbf{k}) \cdot \frac{\mathbf{p}_e}{m_e} | \mathbf{K}_i, n_i \rangle \\ &= \frac{1}{(2\pi)^3} \int d^3\mathbf{X} \exp[i(\mathbf{K}_i - \mathbf{K}_f - \mathbf{k}) \cdot \mathbf{X}] \\ & \quad \times \int d^3\mathbf{x} \psi_f^+(\mathbf{x}) \boldsymbol{\epsilon}_\gamma^+(\mathbf{k}) \cdot \frac{\hbar}{im_e} \frac{\partial}{\partial \mathbf{x}} \psi_i(\mathbf{x}) \\ &= \delta(\mathbf{K}_i - \mathbf{K}_f - \mathbf{k}) \\ & \quad \times \int d^3\mathbf{x} \psi_f^+(\mathbf{x}) \boldsymbol{\epsilon}_\gamma^+(\mathbf{k}) \cdot \frac{\hbar}{im_e} \frac{\partial}{\partial \mathbf{x}} \psi_i(\mathbf{x}). \end{aligned} \quad (\text{C8})$$

Inclusion of the center of mass motion of the atom multiplies the standard transition matrix element with a momentum conserving δ function. The squares of these extra factors cancel in the calculation of observables from the squares $|S_{fi}|^2$ of scattering matrix elements, since the final center of mass momentum $\hbar\mathbf{K}_f$ adds an integration $\int d^3\mathbf{K}_f \dots$, the square of the momentum conserving δ function contributes a factor $(\mathcal{V}/8\pi^3)\delta(\mathbf{K}_i - \mathbf{K}_f - \mathbf{k})$, and the fixed initial center of mass momentum contributes an elementary \mathbf{K} space volume $8\pi^3/\mathcal{V}$, such that the only contribution from inclusion of the center of mass motion is to shift $\mathbf{K}_i \rightarrow \mathbf{K}_f = \mathbf{K}_i - \mathbf{k}$. This shifts energy conservation for spontaneous emission, $E_i(\mathbf{K}_i) > E_f(\mathbf{K}_f)$, from $ck = \omega_{if} = [E_i(\mathbf{K}) - E_f(\mathbf{K})]/\hbar$ to

$$\begin{aligned} ck &= \frac{E_i(\mathbf{K}_i) - E_f(\mathbf{K}_f)}{\hbar} \\ &= \frac{\hbar}{2} \frac{2\mathbf{K}_i \cdot \mathbf{k} - \mathbf{k}^2}{m_p + m_e} + \omega_i - \omega_f. \end{aligned} \quad (\text{C9})$$

The net effect of the atomic recoil is therefore a frequency shift that in leading order in $\hbar|\mathbf{K}_i|/(m_p + m_e)c$ and $\hbar\omega_{if}/(m_p + m_e)c^2$ takes the form (with scattering angle θ)

$$ck = \omega_{if} + \frac{\hbar|\mathbf{K}_i| \cos \theta}{(m_p + m_e)c} \omega_{if} - \frac{\hbar\omega_{if}^2}{2(m_p + m_e)c^2}. \quad (\text{C10})$$

The frequency shift is very small in comparison to ω_{if} if the transition involves nonrelativistic atoms, $\hbar|\mathbf{K}_i| \ll m_p c$. In cases of absorption or scattering, when we have photons in the initial state, we should also exclude high energy γ -rays to neglect atomic recoil effects. However, recall that we have already excluded photons beyond the soft X-ray regime through the use of dipole approximation. We also note that for photons below the hard X-ray regime, possible energy shifts from recoils of quasifree electrons are also suppressed by $\hbar|\mathbf{k}|/m_e c$.

The observation that recoils yield frequency shifts, but do not generate extra factors in transition rates, also applies if the matrix element does not directly connect initial and final atomic states but includes intermediate virtual states. Integration over intermediate virtual center of mass momenta $\hbar\mathbf{K}_v$ only reduces momentum conserving δ functions in $|S_{fi}|^2$ according to

$$\begin{aligned} & \int d^3\mathbf{K}_v \delta(\mathbf{K}_v - \mathbf{K}_f - \mathbf{k}') \delta(\mathbf{K}_i - \mathbf{K}_v + \mathbf{k}) \\ &= \delta(\mathbf{K}_i - \mathbf{K}_f + \mathbf{k} - \mathbf{k}'). \end{aligned} \quad (\text{C11})$$

Appendix D: Photon emission from radiative electron-hole recombination between energy bands

Eqs. (47,50) apply to transitions between conduction bands, but not to a conduction electron filling a valence band hole. Electron-hole annihilation through interband transition requires special considerations because now we are effectively dealing with two particles in the initial state, *viz.* a conduction electron with wave vector $\mathbf{k}_{e,i}$ and a valence band hole with wave vector $-\mathbf{k}_{e,f} = \Delta\mathbf{k} - \mathbf{k}_{e,i}$. Interband electron-hole recombination is therefore akin to two-particle annihilation events that are characterized by annihilation cross sections.

We use subscripts c and v for labeling the conduction band and the valence band, respectively. The initial electron-hole state is then $a_{c,s}^+(\mathbf{k}_{e,i})a_{v,s}(\mathbf{k}_{e,f})|\Omega\rangle$, where the ground state $|\Omega\rangle$ corresponds to the filled Fermi volume in the Brillouin zone, $a_{c,s}^+(\mathbf{k}_{e,i})$ is an electron creation operator in the conduction band, and $c_{v,s}^+(-\mathbf{k}_{e,f}) = a_{v,s}(\mathbf{k}_{e,f})$ acts as a hole creation operator in the valence band [46, 47]. We also assume the same spin projection s for the electron and the hole because the operators (6) preserve spin projections.

The reduction in final state measure due to the initial state $a_{c,s}^+(\mathbf{k}_{e,i})a_{v,s}(\mathbf{k}_{e,f})|\Omega\rangle$, compared to the case in Sec. IID of transition between conduction bands, $d^3\mathbf{k}d^3\mathbf{k}_{e,f} \rightarrow d^3\mathbf{k}$, implies that integration over final states now only takes care of momentum conservation, but an energy-conserving δ -function remains,

$$\begin{aligned} & \delta[ck + \omega_v(\mathbf{k}_{e,f}) - \omega_c(\mathbf{k}_{e,i})] \delta(\mathbf{k} + \mathbf{k}_{e,f} - \mathbf{k}_{e,i}) \\ & \rightarrow \delta[c|\mathbf{k}_{e,i} - \mathbf{k}_{e,f}| + \omega_v(\mathbf{k}_{e,f}) - \omega_c(\mathbf{k}_{e,i})], \end{aligned} \quad (\text{D1})$$

and this constrains the pairs of wave vectors in the Brillouin zone where electron-hole recombination generates single-photon emission as a purely radiative process. Indeed, we should expect kinematic constraints since the corresponding process for free particle-antiparticle pairs is forbidden by energy-momentum conservation. Single-photon emission from electron-hole recombination for generic combinations of wave vectors therefore requires phonon assistance, creation of Auger electrons, assistance through particle traps, or two-photon emission. These mechanisms are outside of the scope of the current review of leading order radiative processes.

For completeness, however, we give a formula that applies to the purely radiative single-photon emission from electron-hole recombination if the constraint (D1) can be satisfied within the linewidth of the transition.

Electron-hole recombination rates are normalized by the differential current density of conduction electrons

$$\frac{d\mathbf{j}_e(\mathbf{k}_e)}{d^3\mathbf{k}_e} = \frac{1}{V} \int_V d^3\mathbf{x} \frac{d\mathbf{J}_e(\mathbf{k}_e, \mathbf{x})}{d^3\mathbf{k}_e}, \quad (\text{D2})$$

which arises from the \mathbf{x} -dependent differential current density of conduction electrons,

$$d\mathbf{J}_e(\mathbf{k}_e, \mathbf{x}) = \psi_c^+(\mathbf{k}_e, \mathbf{x}) \frac{\hbar}{2im} \frac{\partial \psi_c(\mathbf{k}_e, \mathbf{x})}{\partial \mathbf{x}} d^3\mathbf{k}_e - \frac{\hbar}{2im} \frac{\partial \psi_c^+(\mathbf{k}_e, \mathbf{x})}{\partial \mathbf{x}} \psi_c(\mathbf{k}_e, \mathbf{x}) d^3\mathbf{k}_e, \quad (\text{D3})$$

through averaging over the Wigner-Seitz cell. Note that the differential current densities $d\mathbf{J}_e(\mathbf{k}_e, \mathbf{x})/d^3\mathbf{k}_e$ and $d\mathbf{j}_e(\mathbf{k}_e)/d^3\mathbf{k}_e$ have dimensions of velocities, e.g. units of cm/s.

Radiative electron-hole recombination through single-photon emission can then be characterized by a cross section

$$\begin{aligned} \sigma(\mathbf{k}_{e,i}, \mathbf{k}_{e,f}, \epsilon_\gamma) &= \frac{\alpha_S [\omega_c(\mathbf{k}_{e,i}) - \omega_v(\mathbf{k}_{e,f})]^2}{2\pi |\mathbf{k}_{e,i} - \mathbf{k}_{e,f}|} \\ &\times \frac{|\langle u_v(\mathbf{k}_{e,f}) | \epsilon_\gamma^+(\mathbf{k}_{e,i} - \mathbf{k}_{e,f}) \cdot \mathbf{x} | u_c(\mathbf{k}_{e,i}) \rangle_V|^2}{|d\mathbf{j}_e(\mathbf{k}_{e,i})/d^3\mathbf{k}_{e,i}|} \\ &\times \Delta_\Gamma [c|\mathbf{k}_{e,i} - \mathbf{k}_{e,f}| + \omega_v(\mathbf{k}_{e,f}) - \omega_c(\mathbf{k}_{e,i})]. \quad (\text{D4}) \end{aligned}$$

As explained in Eqs. (17) and (19-23), averaging over angles removes dependence of matrix elements on polarization vectors. Here this yields an angle averaged electron-hole recombination cross section from single-photon emission,

$$\begin{aligned} \sigma(\mathbf{k}_{e,i}, \mathbf{k}_{e,f}) &= \frac{\alpha_S [\omega_c(\mathbf{k}_{e,i}) - \omega_v(\mathbf{k}_{e,f})]^2}{6\pi |\mathbf{k}_{e,i} - \mathbf{k}_{e,f}|} \\ &\times \frac{|\langle u_v(\mathbf{k}_{e,f}) | \mathbf{x} | u_c(\mathbf{k}_{e,i}) \rangle_V|^2}{|d\mathbf{j}_e(\mathbf{k}_{e,i})/d^3\mathbf{k}_{e,i}|} \\ &\times \Delta_\Gamma [c|\mathbf{k}_{e,i} - \mathbf{k}_{e,f}| + \omega_v(\mathbf{k}_{e,f}) - \omega_c(\mathbf{k}_{e,i})]. \quad (\text{D5}) \end{aligned}$$

Integration of $\sigma(\mathbf{k}_{e,i}, \mathbf{k}_{e,f})$ against the $\mathbf{k}_{e,i}$ -dependent differential conduction current density $|d\mathbf{j}_e(\mathbf{k}_{e,i})/d^3\mathbf{k}_{e,i}|$ and the $\mathbf{k}_{e,f}$ -dependent differential hole density $|d\rho_h(\mathbf{k}_{e,f})/d^3\mathbf{k}_{e,f}|$ (which is \mathbf{x} -independent if averaged over the Wigner-Seitz cell) then yields an estimate for the photon emission rate per volume for those photons that were generated through purely radiative single-photon electron-hole recombination, i.e. from recombinations that were not assisted through phonon processes or Auger excitations or trapping mechanisms, and that did not result from two-photon emission.

ACKNOWLEDGMENTS

We would like to thank Alexander Moewes, Graham George and Robert Green for encouraging and helpful comments. We acknowledge support from the Natural Sciences and Engineering Research Council of Canada.

-
- [1] A. Messiah, *Quantum Mechanics*, volume 2, North-Holland, Amsterdam (1962).
- [2] J.J. Sakurai, *Advanced Quantum Mechanics*, Addison-Wesley, Reading, MA (1967).
- [3] E. Merzbacher, *Quantum Mechanics*, 3rd edition, Wiley, New York (1998).
- [4] F. Schwabl, *Quantum Mechanics*, 4th edition, Springer, Berlin (2007).
- [5] R. Dick, *Advanced Quantum Mechanics – Materials and Photons*, 3rd edition, Springer Nature, Cham, Switzerland (2020).
- [6] G.W.F. Drake (Editor), *Springer Handbook of Atomic, Molecular, and Optical Physics*, Springer, New York (2006).
- [7] R.C. Hilborn, *American Journal of Physics* **50**, 982–986 (1982).
- [8] Excitations within an energy band and near an extremum could eventually be described through quasiparticles with an effective mass $m_* \neq m$. The advantage of such a quasiparticle description of intraband excitations near an extremum is replacement of the actual energy band $E_n(\mathbf{k}_e)$ with a parabolic band $E_*(\mathbf{k}_e) = E_*(\mathbf{0}) + \hbar^2 \mathbf{k}_e^2 / 2m_*$, and replacement of the electronic Bloch energy eigenfunctions $\psi_n(\mathbf{k}_e, \mathbf{x})$ with plane waves. However, this is not possible for interband transitions that are not confined to extrema with identical effective masses. Please also note that Bloch energy eigenfunctions and energy bands in materials are derived from Hamiltonians (8) with $m = m_e$, not from Hamiltonians containing effective masses. Stated differently, electrons in energy bands in materials are still electrons, not quasielectrons. The situation is not different from electrons in other complex many-electron systems like many-electron atoms or molecules.
- [9] The “total” emission rates can still be differential emission rates with respect to energy intervals dE or \mathbf{k}_e -space volume elements $d^3\mathbf{k}_e$ if continuous electronic states are involved in the transition.
- [10] We write $\psi_n(\mathbf{k}_e, \mathbf{x}) = \langle \mathbf{x} | n, \mathbf{k}_e \rangle$ for the wave function of the state $|n, \mathbf{k}_e\rangle$.
- [11] V. Weisskopf and E. Wigner, *Zeitschrift für Physik* **63**, 54–73 (1930).
- [12] G. Scala, K. Slowik, P. Facchi, S. Pascazio, and F.V. Pepe, *Physical Review A* **104**, 013722 (2021).
- [13] I. Waller, *Zeitschrift für Physik* **51**, 213–231 (1928).
- [14] P.A.M. Dirac, *The Principles of Quantum Mechanics*, 2nd edition, Oxford University Press, Oxford, UK (1935).

- [15] W. Heitler, *The Quantum Theory of Radiation*, Oxford University Press, Oxford, UK (1936).
- [16] J. Tulkki and T. Åberg, *Journal of Physics B* **13**, 3341–3360 (1980).
- [17] F. Gel'mukhanov and H. Ågren, *Physics Reports* **312**, 87–330 (1999).
- [18] V. Weisskopf, *Annalen der Physik* **401**, 23–66 (1931).
- [19] V.B. Berestetskii, L.P. Pitaevskii, and E.M. Lifshitz, *Quantum Electrodynamics*, 2nd edition, Pergamon Press, Oxford, UK (1982).
- [20] Y. Ma, N. Wassdahl, P. Skytt, J. Guo, J. Nordgren, P.D. Johnson, J.-E. Rubensson, T. Boske, W. Eberhardt, and S.D. Kevan, *Physical Review Letters* **69**, 2598–2601 (1992).
- [21] Y. Ma, *Physical Review B* **49**, 5799–5805 (1994).
- [22] S. Eisebitt and W. Eberhardt, *Journal of Electron Spectroscopy and Related Phenomena* **110–111**, 335–338 (2000).
- [23] E.L. Shirley, *Journal of Electron Spectroscopy and Related Phenomena* **110–111**, 305–321 (2000).
- [24] L.J.P. Ament, M. van Veenendaal, T.P. Devereaux, J.P. Hill, and J. van den Brink, *Reviews of Modern Physics* **83**, 705–767 (2011).
- [25] P. Glatzel, Tsu-Chien Weng, K. Kvashnina, J. Swarbrick, M. Sikora, E. Gallo, N. Smolentsev, and R.A. Mori, *Journal of Electron Spectroscopy and Related Phenomena* **188**, 17–25 (2013).
- [26] F. Gel'mukhanov, M. Odelius, S.P. Polyutov, A. Föhlisch, and V. Kimberg, *Reviews of Modern Physics* **93**, 035001 (2021).
- [27] F.M.F. de Groot, *Physical Review B* **53**, 7099–7110 (1996).
- [28] A. Moewes, S. Stadler, R.P. Winarksi, D.L. Ederer, M.M. Grush, and T.A. Callcott, *Physical Review B* **58**, R15951–R15954 (1998).
- [29] A. Moewes, A.V. Postnikov, E.Z. Kurmaev, M.M. Grush, and D.L. Ederer, *Europhysics Letters* **49**, 665–671 (2000).
- [30] M. Taguchi, L. Braicovich, G. Ghiringhelli, A. Tagliiferri, F. Borgatti, C. Dallera, K. Giarda, and N.B. Brookes, *Physical Review B* **63**, 235113 (2001).
- [31] A. Moewes, T. Eskildsen, D.L. Ederer, J. Wang, J. McGuire, and T.A. Callcott, *Physical Review B* **57**, R8059–R8062 (1998).
- [32] A. Moewes, D.L. Ederer, M.M. Grush, and T.A. Callcott, *Physical Review B* **59**, 5452–5456 (1999).
- [33] A. Moewes, M.M. Grush, T.A. Callcott, and D.L. Ederer, *Physical Review B* **60**, 15728–15731 (1999).
- [34] A. Hunt, D. Muir, and A. Moewes, *Journal of Electron Spectroscopy and Related Phenomena* **144–147**, 573–576 (2005).
- [35] J. Jiménez-Mier, J. van Ek, D.L. Ederer, T.A. Callcott, J.J. Jia, J. Carlisle, L. Terminello, A. Asfaw, and R.C. Perera, *Physical Review B* **59**, 2649–2658 (1999).
- [36] M. Magnuson, S.M. Butorin, J.-H. Guo, and J. Nordgren, *Physical Review B* **65**, 205106 (2002).
- [37] Ru-Pan Wang, B. Liu, R.J. Green, M.U. Delgado-Jaime, M. Ghiasi, T. Schmitt, M.M. van Schooneveld, and F.M.F. de Groot, *Journal of Physical Chemistry C* **121**, 24919–24928 (2017).
- [38] A. Kikas, T. Käämbre, A. Saar, K. Kooser, E. Nömmiste, I. Martinson, V. Kimberg, S. Polyutov, and F. Gel'mukhanov, *Physical Review B* **70**, 085102 (2004).
- [39] J. Szlachetko, J.-Cl. Dousse, J. Hozzowska, M. Pajek, R. Barrett, M. Berset, K. Fennane, A. Kubala-Kukus, and M. Szlachetko, *Physical Review Letters* **97**, 073001 (2006).
- [40] J. Szlachetko, J.-Cl. Dousse, M. Berset, K. Fennane, M. Szlachetko, J. Hozzowska, R. Barrett, M. Pajek, and A. Kubalas-Kukus, *Physical Review A* **75**, 022512 (2007).
- [41] L. Zhang, N. Schwertfager, T. Cheiwchanchamnangij, X. Lin, P.-A. Glans-Suzuki, L.F.J. Piper, S. Limpijum-nong, Y. Luo, J.F. Zhu, W.R.L. Lambrecht, and J.-H. Guo, *Physical Review B* **86**, 245430 (2012).
- [42] A.R.H. Preston, A. DeMasi, L.F.J. Piper, K.E. Smith, W.R.L. Lambrecht, A. Boonchun, T. Cheiwchanchamnangij, J. Arnemann, M. van Schilfgaarde, and B.J. Ruck, *Physical Review B* **83**, 205106 (2011).
- [43] S.I. Bokarev, M. Dantz, E. Suljoti, O. Kühn, and E.F. Aziz, *Physical Review Letters* **111**, 083002 (2013).
- [44] R.J. Green, D. Peak, A.J. Achkar, J.S. Tse, A. Moewes, D.G. Hawthorn, and T.Z. Regier, *Physical Review Letters* **112**, 129301 (2014).
- [45] L. Kjellsson, V. Ekholm, M. Agåker, C. Sätze, A. Pietzsch, H.O. Karlsson, N. Jaouen, A. Nicolaou, M. Guarise, C. Hague, J. Lüning, S.G. Chiuzbăian, and J.-E. Rubensson, *Physical Review A* **103**, 022812 (2021).
- [46] C. Kittel, *Quantum Theory of Solids*, 2nd revised printing, Wiley, New York (1987).
- [47] However, as pointed out already in note [8], we cannot in general use a hole quasifermion picture for interband transitions, but still have to use the electronic Bloch wave function for the missing electron.